IDENTIFICATION OF FUNGAL INFECTION IN WHEAT USING THERMAL IMAGING TECHNIQUE

BY

CHELLADURAI VELLAICHAMY

A thesis Submitted to
the Faculty of Graduate Studies
in Partial Fulfillment of the Requirements
for the Degree of

MASTER OF SCIENCE

Department of Biosytems Engineering
University of Manitoba
Winnipeg, Manitoba

THE UNIVERSITY OF MANITOBA

FACULTY OF GRADUATE STUDIES

*****

COPYRIGHT PERMISSION

IDENTIFICATION OF FUNGAL INFECTION IN WHEAT USING THERMAL IMAGING TECHNIQUE

BY

CHELLADURAI VELLAICHAMY

A Thesis/ Practicum submitted to the Faculty of Graduate Studies of the University of Manitoba in partial fulfillment of the requirement of the degree

of

MASTER OF SCIENCE

Abstract

Wheat is the major cereal crop grown in Canada, and about 70% of its production is exported to various countries. Growth of fungi on the grain is the most common cause of spoilage of stored grain. The traditional fungal detection methods such as plate agar and microscopic detection techniques require about a week for detection and quantification. Early detection of fungal infection is necessary to carry out control methods to minimize the storage losses. The feasibility of the infrared thermal imaging system to identify the fungal infection in stored wheat was studied.

Thermal images of bulk wheat grains infected by *Aspergillus glaucus, Aspergillus niger* and *Penicillium* spp. were obtained using an un-cooled focal planar array type infrared thermal camera after heating grain with a plate heater and cooling in ambient air for 180 and 30 s, respectively. In total, twelve temperature features were derived from heating and cooling data. Ten-way, three-way, pair-wise and infection level based classification models were developed by linear and quadratic discriminant analyses using the derived temperature features.

Classification accuracies of 90-100% and 95.5-99% were obtained for healthy and fungal-infected samples, respectively, using pair-wise linear discriminant analysis (LDA) classifier from a three-week old infection. In quadratic discriminant analysis (QDA), classification accuracies were 86-100% and 94.5-98.69% for healthy and infected samples, respectively. In pair-wise comparisons between healthy and for each of the fungal species infected samples, the LDA classifier yielded an accuracy of >91% for healthy, >95% for *A. glaucus*-infected, and >94% for *A. niger*-infected samples from the

3rd week of infection onwards. When classifying *A. glaucus*, *A. niger* and *Penicillum*-infected grains at different infection periods, both classifiers gave relatively low accuracies (25 to 71.9%) for leave-one-out and bootstrapping validation methods. Most of the misclassification happened between the fungal species at the same level of infection.

The early detection of fungal infection, i.e., at 3 weeks of fungal growth helps to carry out the control measures to prevent the grain deterioration and quality loss. The results prove that the thermal imaging system has the potential for application in the grain industry to detect the kernels infected by fungi and the level of infection (low or high).

Acknowledgments

I express my deep sense of gratitude and hearty thanks to Dr. Digvir S. Jayas, Associate Vice-President (Research), University of Manitoba, for giving me the great opportunity to work on this project, valuable guidance, timely suggestions, and constant support throughout the period of my study. I also express my heartfelt thanks to Dr. Noel D.G. White, Senior Research Scientist, Agriculture and Agri-Food Canada, Winnipeg, for his valuable technical advice and endless help during this study. I thank Dr. Rob Currie, Associate Professor, Department of Entomology, University of Manitoba, for serving on my advisory committee and reviewing my research work.

I thank C.J. Demianyk for helping me in the sample preparation, Matt McDonald for his technical support, and Debby Watson and Evelyn Fehr for their administrative support. On a special note, I express my gratitude to Dr. Manickavasagan Annamalai, Scientist, Mccain Foods, and Mr. Mahesh Sivakumar for their help and technical advice over the past two years.

I would like to thank my fellow researchers Chandra Bhan Singh, Dipali Shridhar Narvankar, Dr. Prabal K. Ghosh, Dr. Ruplal Choudhary, Feng Wang, Ganesan Ramalingam, Gayathiri Pichai, Hai Yan Li, Jun Wu, Ke Sun, Nithya Udayakumar, Rajarammanna Ramachandran, Russ V. Parker, Sathya Gunasekaran,

Senthilkumar Thiruppathi, Sujala Balaji, Sureshraja Neethirajan, Vadivammbal Rajagopal and Wenyu Zhang for their help during the course of my studies.

I thank the Natural Sciences and Engineering Research Council of Canada and Canada Research Chairs program for the financial support for this study.

I express my hearty thanks to my parents, and my friends for their love and moral support throughout the period of my study.

Dedicated to my parents and teachers...

TABLE OF CONTENTS

List of Tables

List of Figures

Chapter 1

INTRODUCTION

Wheat is the second most commonly produced food crop among all cereal crops, after maize (FAS 2007). Canada is the sixth largest producer and the second largest exporter of wheat in the world. In 2006 - 07, Canadian wheat production and export were 27.28 Mt and 19.51 Mt, respectively (FAOSTAT 2007). Every year, nearly 10 to 30% of produced grains are lost throughout the world due to insect and fungal activities (White 1995). It has been estimated that, around 5 to 10% of global food loss is caused by mold activities annually. Fungal growth causes many undesirable changes such as discoloration of grains, production of undesirable odors, reduction of germination and dry matter content, production of hot spots in storage silos, and increase of free fatty acids in stored grain. Sometimes, fungal infection in grains and their products leads to production of mycotoxins, which are harmful to humans and animals after consumption (Tseng et al. 1995). Appearance is one of the most important factors in grain grading. Discoloration and quality loss happen in the stored grain due to fungal growth, and it decreases the market value of the grain.

Fungal species that attack cereal grains can be broadly classified into two groups: pre-harvest or field fungi and post-harvest or storage fungi. Field fungi generally cause minor damage to grains and can be eliminated by proper drying processes before storage. Post-harvest or storage fungi affect grains during storage, kill the seed, and continue to grow at favourable moisture content and storage temperature. Maximum mold growth occurs at 30 to 35°C and >15% moisture content (Muir and White 2001). In Canada, the major post-harvest fungi in wheat are *Aspergillus* spp. (blue, green, yellow, black, white, and brown) and *Penicillium* spp. (blue). The required water activity and storage temperature range for *Aspergillus* spp. growth are 0.65 and -8 to 58°C, respectively, and for *Penicillium* spp. the same are 0.80 and -4 to 48°C, respectively. Optimum water activity and storage temperature range for most storage fungal species are 0.95 to 0.99 and 20 to 40°C, respectively. Some of the *Aspergillus spp.* and *Penicillium* spp. fungi can produce mycotoxins in stored grains. An early detection of fungal infection helps to initiate control measures before the commencement of grain deterioration.

Traditionally, microbial culture methods are used to detect fungi in grain and other raw materials, which require a long time for enumeration and quantification (Keshri et al. 1998). Effect on the degradation of grain chemical components (Magan 1993), respiratory activity of the molds (Lacey et al. 1994), biochemical markers such as ergosterol (Tothill et al. 1992), and fungal enzyme activity (Jain et al. 1991) have been used for examining fungal infection in grains. Ultrasound (Walcott et al. 1998), electronic nose (Keshri et al. 1998), near-infrared spectroscopy (Pearson et al. 2001; Dowell et al. 2002; Wang et al. 2003), and near-infrared hyperspectral imaging technique (Singh et al. 2007) were also tested for detecting fungi in grains. These methods produced good

results for high levels of fungal infection, but could not detect easily low levels of infection. Identification of different fungal species in stored wheat is also a problem with these methods.

Thermal imaging technique has been widely used in civil engineering, electrical and manufacturing industries (Agerskans 1975). In agricultural sciences, this technique has been used for a wide range of applications such as quality evaluation of fruits and vegetables (Varith et al. 2003), measurement of maturity, size and number of fruits on trees for mechanical harvesting (Danno et al. 1980), detection of plant viruses (Chaerle et al. 1999), detection of spoilage due to microbial activities (Hellebrand et al. 2002) and prediction of yield from a farm (Stajnko et al. 2004). Also, it has been used to study the physiology of the plants and plant water relationships, which is helped to schedule irrigation (Jones 1999). Similarly, it has been used for various grain handling operations such as wheat class identification, detection of insect infestation, and quantification of non-uniform drying of cereal grains and oil seeds during microwave heating (Manickavasagan 2007; Vadivambal et al. 2007).

In thermal imaging, the temperature radiation pattern of an object which is invisible to the human eye is converted into a visible two dimensional thermal image. The amount of radiation emitted by an object increases with temperature, therefore, thermal imaging allows to see the variations in temperature. A thermal camera is used to collect and convert the thermal infrared radiation emitted by objects into images that can be seen on a view screen or computer display (Davis and Lettington 1988). In the electromagnetic spectrum, the region between 3 and 14 μm is called the thermal infrared region, and the heat signature applying imaging techniques uses this band for imaging applications

(Gonzalez and Woods 2002). The thermal imaging technique is a potential method for the remote detection of abnormality in agricultural products based on the temperature changes during heating and cooling (Manickavasagan 2007). Therefore, the objectives of this study were:

1. to assess the potential of infrared thermal imaging to identify fungal infection in wheat, and
2. to develop statistical classification models to classify the fungal infection at different infection levels.

Chapter 2

REVIEW OF LITERATURE

2.1 Basics of Thermal Imaging

Thermography, or thermal imaging, is a type of infrared imaging. It works on the principle that any object having a temperature above absolute zero (-273.15°C) emits electromagnetic radiation which is invisible to the naked human eye. This heat or thermal radiation occupies approximately 900–14,000 nm in the electromagnetic spectrum (Fig. 2.1). It deals with the infrared spectral band between optical red and microwave wavelengths. The infrared thermograph or a thermal image is a "picture" of heat of an object. The thermal camera converts the surface temperature of an object to a visible two dimensional image. As the infrared radiation is emitted by all objects based on their temperatures, thermal imaging makes it possible to "see" one's environment with or without visible illumination based on the black body radiation law. The amount of radiation emitted by an object increases with temperature, so that thermal imaging allows us to see the variations in temperature. A thermal camera can collect and convert the

thermal infrared radiation emitted by objects into images that can be seen on a view screen or a computer display.

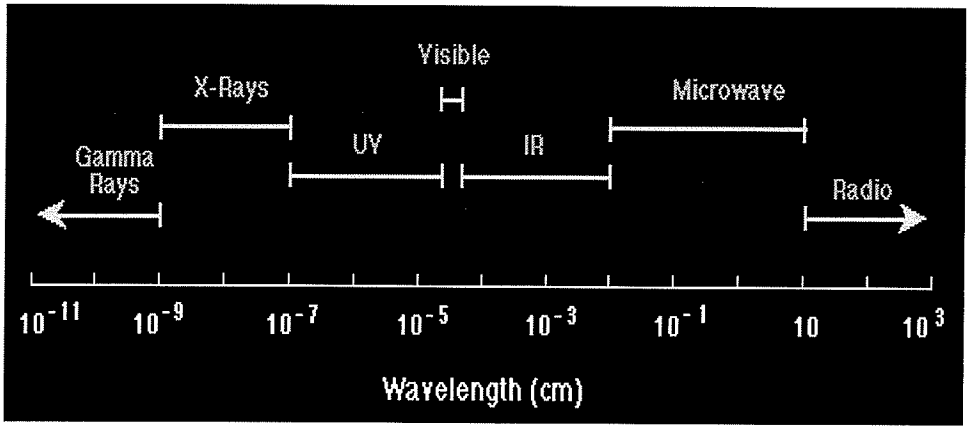

Figure 2.1 Electromagnetic spectrum (Source: Anonymous, 2007)

The commercial infrared thermal cameras work in any of the following wavelength bands and their filtered sub-bands (Anonymous 2007).

1. Near infrared band (0.7 to 1.7 microns),
2. Short wave (SW) band (1.8 to 2.4 microns),
3. Medium wave (MW) band (2.4 to 5 microns), and the
4. Long wave (LW) band (8 to 14 microns).

The short and long wavelength regions have good transmission in the atmosphere, so these two wave bands are used for radiation measurement.

2.1.1 Radiation laws

In the second half of the 19th century, it was known that heat radiation and other electromagnetic waves, such as visible light or radio waves, were similar in nature. This was followed by the discovery of the laws of radiation by Kirchhoff, Stefan-Boltzmann, Wien and Planck. By the mid-20th century, infrared thermography was intensively used

for military purposes and first thermographic devices for non-military application were invented in the 1960s.

The object that emits all of the absorbed radiation is known as the "black body". The spectral spread of radiation emitted by a black body is described by Planck's radiation law (Touloukian and DeWitt 1972):

$$M_\lambda = \frac{2\pi hc^2}{\lambda^5[\exp(hc/k\lambda T) - 1]} \qquad (2.1)$$

where,

M_λ = Energy per unit area per unit wavelength (W m^{-2} μm^{-1})

λ = Wavelength (μm)

T = temperature of the object (K)

h, c and k are constants

Planck's radiation law represents the principal correlation of non-contact temperature measurements. Due to its abstract nature, however, it cannot directly be applicable in this form for many practical calculations. Stefan-Boltzmann's and Wein's laws are derived from Planck's law. By integrating the spectral radiation intensity across all wavelengths, the value of the entire radiation emitted by the body is obtained. This correlation is called the Stefan-Boltzmann's law (Touloukian and DeWitt 1972):

$$M = \sigma \varepsilon T^4 \qquad (2.2)$$

where :

σ = Stefan – Boltzman constant = 5.67×10^{-8} (W m^{-2} K^{-4})

M = total amount of radiation emitted per unit area (W m^{-2})

ε = emmisivity of the object, and

T = temperature of the object (K)

The Stefan-Boltzmann's law (Eqn 2.2) shows that total amount of thermal radiation emitted by an object is dependent on emissivity and temperature of the object allowing the temperature of the object to be calculated. The emissivity of an object is important for the quantitative temperature measurement, but for qualitative differentiation emissivity can be neglected (Hellebrand et al. 2002).

2.1.2 Influence by the measuring distance

Since infrared thermography is a non-contact procedure, infrared radiation needs to travel over a certain distance between the object to be measured (sample) and the measuring device (thermal camera) through a medium whose infraoptical properties may affect the measured result. In most cases, this medium is likely to be atmospheric air, but also other materials, such as infrared-transmittant "windows" also occur in real life. In the case of air, these are mainly its components, such as water vapour and carbon dioxide, which may affect the infrared transmittance (Gaussorgues 1994).

The level of transmittance of air is strongly dependent on wavelength. At the long-wave atmospheric window (8-14 μm), the level of transmittance remains equally high over longer distances, and at the short-wave atmospheric window (3-5 μm), the

measurable transmittance decrease caused by the atmosphere occurs at distances of some ten meters (Wolfe and Zissis 1978).

2.1.3 Influence by the measured object

The black body as a radiometric model is indispensable when considering principal correlations. Since real objects, that are to be measured, deviate more or less strongly from that model, it may become necessary to take this influence into account in measurements. Especially suited for this purpose is the parameter of emittance which is the measure for a body's capability of emitting infrared radiation. Having a value of 1, the black body has the highest possible emittance, which is additionally dependent on wavelength (Gaussorgues 1994). Contrary to this, the emittance of real objects to be measured may show more or less strong dependence on wavelength. The following parameters may also be of some influence:

1. Material composition
2. Oxide film on the surface
3. Surface roughness
4. Angle to the surface normal
5. Temperature
6. Polarisation degree

A multitude of non-metallic materials at least within the long-wave spectral range show high and relatively constant emittance, regardless of their surface structure. In

contrast, metals generally have low emissivity that greatly depend on the surface properties and drop as wavelengths increase (Touloukian and DeWitt 1972).

2.2 Applications of Thermal Imaging in Agricultural Sciences

2.2.1 Quality evaluation of fruits and vegetables

Detection of defect, bruise and damage in fruits and vegetables are the most common problems during harvesting and transportation operations. Due to mechanical damage and lack of effective quality measurement systems, the apple industry loses millions of dollars every year. Apple bruises are difficult to detect by visual or automatic color sorting systems because bruising takes place beneath the peel. Thermocam PM390 with 3.4 - 5 μm spectral band system was used for acquiring thermal images of apples during: (a) heating with ambient air at 26°C; (b) heating with forced convection in the same air heated to 37°C and; (c) cooling with forced convection ambient air at 50% RH, 26°C after heating in 40°C water for 2-3 min (Varith et al. 2003). At steady state condition, there were no temperature differences between bruised and sound tissues. The bruise detection efficiency of Fuji and McIntosh apples at 3°C warmed by air at 26°C was 100% within 180 s or less and air at 37°C gave 86.7-100% efficiency. The bruise detection works because the thermal diffusivity is different between a bruised and sound tissues. While heating the fruits by air, bruises warmed more slowly than sound tissues.

An Infra-Eye 102A with a spectral range of 8-14 μm was used to detect bruises in apple, Satsuma mandarin and Natudaiadai fruits. The surface temperature of the

bruised fruits were lower by 0.3 - 1.0°C, 0.2 - 0.8°C and 0.3 - 0.8°C than that of unbruised apple, Satsuma mandarins and Natsudaidai fruits, respectively (Danno et al. 1978).

Maturity grading of tomato, Japanese persimmon and Japanese pear was evaluated using the Infra-Eye 102A thermography system (Danno et al. 1980). The surface temperature of the immature fruits and vegetables was slightly higher than the mature and over-ripe ones when stored at lower temperature before imaging and slightly lower when stored at higher temperature before measurement.

Surface quality and wax layer structure of apple fruits were measured by thermal imaging. Thermal images of two different cultivars of apple ('Jonagored' and 'Elshof') picked at two different dates were obtained by Thermocam SC 3000 for emissivity and individual fruit measurements. An AVIO Compact thermo (TVS-2000 mkll series) fixed above a wind tunnel was used for acquiring thermal images of fruits stored at two different storage conditions. The emissivity of the apple was 0.96 and cooling rate of 'Elsof' apple was higher and had lower surface temperature than 'Jonagored' apple. But thermal imaging could not detect the wax structure changes during storage (Veraverbeke et al. 2003).

The effects of different post-harvest storage conditions on the quality of sweet pepper were studied by non-destructive infrared thermal imaging (Zsom et al. 2005). Thermal images of packed and unpacked sweet peppers stored at two different temperatures were acquired at 5 min intervals for 1 h duration and water transpiration features were calculated using the mean surface temperature of the pepper samples. The

transpiration rate of low density poly ethylene (LDPE) packed fruits stored at 10°C were higher than the other samples due to better physiological conditions of the sample.

2.2.2 Estimation of number and diameter of apple fruits

Prediction of number and size of fruits helped to calculate the future yield and income. At present, European countries only accept the 'Pronogfruit' forecast model for quality and quantity estimation of fruits. This method predicts 97-98% of future yield in large areas. But it is impossible to predict the future yield in small areas like individual orchards and takes a long time for measurement. Stajnko et al. (2004) developed an algorithm using the thermal images acquired from an orchard at different stages of fruit development for estimation of quality and quantity of apple fruits in orchards. They obtained correlation coefficients from 0.83 to 0.88 for number of fruits in a tree and 0.67 to 0.70 for diameter of fruit at different fruit developmental stages.

2.2.3 Plant evaluation by thermal imaging

Commonly spectral signatures and image processing of visible, near infrared and middle infrared images are used for remote recognition and evaluation. Fungal infections in plants were detected by the thermal imaging system (Nilsson 1995). The fungal plant diseases affect the metabolism of the host plant and may change the transpiration rate of the plant. Wheat plants infected by powdery mildew disease were studied using a thermal camera (THERMOCAM SC 500, FLIR systems). Fungal-infected plants produced a higher temperature (0.2 - 0.7K) than the healthy and the temperature differences increased with the course of infection in wheat plants (Hellebrand et al. 2006).

2.2.4 Monitoring plant virus interaction

Plants can show resistance to some pathogens. The resistance to the tobacco mosaic virus (TMV) was monitored by a thermal imaging system before any visible disease symptoms on the plant leaves (Chaerle et al. 1999). Higher temperatures on the places of infection were observed from the thermal images 8 h before the visible cell death. Plants produce salicylic acid (SA) as a inducible resistance to the pathogens which causes metabolic heating and increases the leaf temperature. These incompatible plant-pathogen interactions increase the temperature of the virus-infected portions of the leaf.

2.2.5 Measurement of seedling viability and quality

Viability of the 1 year old 'Scots pine' (*Pinus sylvestris* L.) and 2 year old 'Norway spruce' (*Picea abies (L.) Karst.*) seedlings were determined using the thermography method (Egnell and Orlander 1993). The warmer seedlings had a lower survival rate than the cooler seedlings and a significant negative correlation was found during the first growing year between seedling temperature difference and annual height increment.

Healthy transplants with good genetic, physiological properties are required for easy transplantation to field and higher yield of crops. Invisible quality parameters like photosynthetic rate, chlorophyll content, and root activity were measured by the thermal imaging technique (Kim and Lee 2004). From 11 days to 20 days after stem cutting, leaf temperature of potato transplants were measured once a day by a thermal camera. Leaf temperature of the potato transplants grown in 50 $\mu mol.m^{-2}s^{-1}$ photosynthetic photon flux (PPF) solution was higher than that of transplants grown at 150 and 250 $\mu mol.m^{-2}s^{-1}$ PPF

solutions. Low photosynthesis rate due to the low PPF and water deficiency caused the higher temperature in the potato transplants.

2.2.6 Measurement of plant-soil-water relationship

It is essential to find out the crop stresses as early as possible because the various biotic and abiotic stresses such as insufficient water or nutrient, adverse climatic conditions, plant diseases and insect damage have a negative effect on the crop yield. Jones (1999) used the thermography technique for irrigation scheduling by measuring the stomatal closure as an indicator of plant water stress. Leaf temperatures of runner bean plants were taken by a scheduler crop stress monitor with 2.5° angle of view and 8-14 μm spectral view. The stomatal closure was calculated using leaf temperature and meteorological data in a model. Infrared thermometry was also used to measure the crop stress indices of cotton plants (Inoue 1990). Stomatal closure and transpiration were calculated by a model using the canopy temperature measured by a handheld thermal camera and meteorological data and compared with porometer measured crop indices. The crop stress indices calculated using the thermometry measurements were linearly related with porometer measurements and the coefficient of determinations (R^2) were 0.93 and 0.79 for stomatal closure and transpiration rate. Crop water stress of wheat plants were measured by a remote infrared thermography technique (Berliner et al. 1984). The canopy temperatures of the plants were measured by a thermal camera fixed at 3.3 m height. The stomatal closure and water potential had a linear relationship with the canopy temperature of the crop and the R^2 were 0.64 and 0.65, respectively. Stomatal closure of the grapevine was measured by thermometry using the canopy temperatures (Jones et al.

2002). Predawn water potential of the grapevine crop was significantly different ($p < 0.01$) between irrigated and non-irrigated treatments and also results showed that not only leaf temperature but also the temperatures of other surfaces within the canopy were dependent on the water relations of the crop. A model for estimating the evaporation from pasture was developed using the infrared thermal imaging method (Kalma and Jupp 1990). Quantification of changes in temperature with respect to various plant parameters gave the valuable information required for precision farming. Inoue (1990) used the infrared thermography method to determine the physiological status of stressed and non-stressed wheat and corn canopies. Thermal images of non-stressed and root-reduced crop canopies were taken at every 30 min from a distance of 5 m and 20 m for wheat and corn, respectively. It was observed that a maximum mean temperature difference was not less than 4.1°C and 3.1°C for wheat and corn, respectively. Water status of the wheat crops were measured by the thermometry method along with ground based hyper spectral measurements for nitrogen status in the filed (Fitzgerald et al. 2006). Models developed from the thermometry measured canopy temperature and Canopy Chlorophyll Content Index (CCCI) yielded an R^2 of 0.68.

2.2.7 Thermographic investigations of flower ovens

The thermogenic group of plants such as, *Arum maculatum*, *Arum italicum* and *Victoria cruziana* show a strong increase in metabolic rate during blooming which is used to heat up the flowers. Temperature distribution in various part of the *V. cruziana* flower blossoms grown in the Berlin botanical garden in the year 2000 was obtained using thermography method and compared with the metabolic activities of the different plant

materials (Lamprecht et al. 2002a) . Thermal images of *V. cruziana* buds, blossoms and leaves gave a maximum temperature difference of 9.5 K against the air. The upright rim of the leaves was always 2-3 K cooler than the main parts of the leaves. Plant structures nearer to the floral chamber had higher metabolic rates and a temperature increase of 10 K was observed for the outer parts of the flower like sepals.

Heat production rate of three thermogenic plants, the elephant foot yam (*Amorphophallus paeoniifolius*), the voodoo lily (*Sauromatum guttatum*) and the tropical water lily (*Victorioa cruzizna*) were investigated by infrared thermometry during their metabolic explosion (Lamprecht et al. 2002b). Fertile female florets of *A. paeoniifolius* below the male ones were 2.6 K warmer than air and in *S. guttatum* flowers, heat production rate increased up to 10 K within 40 min during night times.The central plate above the floral chamber of *V. cruziana* flowers was the main place of heat production and it warmed about 9.5 K above the air temperature.

2.2.8 Detection of foreign materials

An infrared thermal imaging system was used to detect foreign materials like rotten nuts, hard shells, and stones in hazelnuts (Meinlschmidt and Margner 2003). Thermal images taken from the process line (conveying belt) were used to develop the algorithms for detection of these foreign materials using histogram analysis, texture analysis and object-oriented image process techniques. The physical behaviour of the food and foreign material, their form and the amount of noise in the thermal images affected the accuracy of the detection models.

2.3 Applications in Health Science

Even though, thermal imaging systems were designed originally for military and industrial uses, the advances in digital system hardware and analytical software allowed using this imaging system for medical applications. Computer-assisted thermography made it simpler and placed it in an inevitable place in medical applications. The temperature of a human body has been an interest of study for more physicians, because the temperature rise produced by metabolic heat producing processes and internal thermoregulatory mechanism is used as a major indicator of diseases. The mean temperature of human body is around 37±1°C at rest, a state of hypothermia exists when the internal temperature falls below 35°C and high temperatures (40 - 41°C) are seen during fever and heat illness. The skin plays an important role in maintaining thermal equilibrium through heat energy exchange process. Major factors influencing the skin temperature are: age, obesity, the environment, exercise and the effects of underlying vasculature on temperature patterns (Jones et al. 1988).

2.3.1 Assessment of inflammatory conditions

Since heat is one of the classical symptoms of inflammation, infrared thermal imaging system was used to assess the localized inflammation and evaluate the treatment (Collins et al. 1974). A quantitative measurement, thermographic index (TI), was calculated using the isotherm temperature recorded by thermography. For healthy subjects the TI values were below 2.5, whereas for inflammatory joints the TI values were raised to 6.0. These values had also been used to assess the effect of anti-inflammatory drugs. Bowel ischemia is a medical condition in which inflammation and

injury of the small intestine result from inadequate blood supply and it causes reduced blood flow. Thermal imaging system had been used for detecting bowel ischemia and showed 100% sensitivity to predict death of cells due to this disease and 69.5% positive prediction value (Brooks et al. 2000).

Thermal imaging system had been used for determining the inflammatory state of Graves' ophthalmopathy disease affected patients and follow-up effect of methylprednisolone pulse therapy to those patients (Chang et al. 2008). Temperature of the orbit of the eye decreased significantly after treatment and the temperature differences were positively correlated with the changes in clinical activity score (correlation coefficient = 0.80).

Ivanitsky et al. (2005) compared the thermal imaging systems operating in wavelength ranges of 3-5 μm and 8-12 μm used for medical diagnosis assessment. Thermal images were taken by both the systems for the patients with different pathologies of the leg and found that the thermal cameras operating in the range of 3-5 μm were more sensitive to the reflexes of skin exposured to external source of heat radiation and the cameras operating in 8-12 μm range showed less effect to lighting units.

2.3.2 Assessment of pain and trauma

Thermal camera has been used to study the temperature differences in the surroundings of tissues for nerve damage (Brelsford and Uematsu 1985). Temperatures were measured in 37 segmental areas of the body using the thermal imaging system and average temperature differences were calculated. For normal controls the average temperature difference between the sides of the body were small (0.17-0.58°C), but in the

case of nerve-damaged patients, the skin temperatures on the impaired nerve side had a difference of 1.63±1°C from that of normal body. In completely sectioned nerves cases, the anesthetic area was 2-4° C warmer than the surrounding skin area.

The infrared thermal imaging system was used to study the effect of transcutaneous electrical stimulation on the skin temperature in the patients with chronic pain (Abram et al. 1980). The temperatures of the thumb of the patients were taken after electrical stimulation for 20-40 min and found that, the temperature increased by 2.5±0.7°C during stimulation in patients who experienced relief of pain, but there were no significant skin temperature changes in patients who experienced zero relief.

2.3.3 Assessment of arterial disease

Thermography had been used to study the effects of sympathetic nerve block to improve the blood flow rate. Thermal images were taken before and after a sympathetic nerve block in the feet, and they found that the sympathetic nerve block increased the skin temperature by 5°C. Amputation of an affected limb is necessary due to the peripheral arterial disease. Infrared thermography had been used to produce some useful physical data such as skin blood flow, perfusion pressure, and arterial pressure gradients, and used for determining the best site of amputation (Jones and Avery 1989).

2.3.4 Oncological investigations

In oncology, a thermal imaging system had been used as an adjunct tool to diagnose malignant diseases and assess disease prognosis. Temperature increases of 2-3°C were found over a known malignant tumour on the skin (Bourjat et al. 1975).

Cristofolini et al. (1976) also found a temperature increment of 1-4°C on the malignant melanomas. Turco et al. (1982) found small temperature elevations due to soft tissue tumours. Amalric et al. (1978) used thermography to diagnose breast cancers and found that the skin surface overlying malignant tumours was 1-4°C warmer than the surrounding skin. Thermographic technique had been used with Complementary Learning Fuzzy Neural Network (CLFNN) to detect breast cancer (Tan et al. 2007). This new model gave prediction accuracies of 94.74%, 84%, and 88% for breast cancer detection, breast tumor detection and breast tumor classification, respectively. Thermography had been used to determine the vascularity of primary bone tumours which resulted in more than 4° C temperature increment (Jones et al. 1975).

Thermal imaging system was also used to monitor the activity of a tumor during treatment and the effects of treatment therapy. Steroid therapy and chemotherapy for breast tumors reduced the surface temperature by 1-3°C (Stoll 1974) and a temporary reduction after treatment followed by a temperature elevation of 2-3°C due to a still active tumor was recorded in radiotherapy (Gros and Gautherie 1980).

2.4 Applications in Animal Science

Infrared thermography had been used to investigate the physiology of energy utilization in pig production (Dauncey and Ingram 1983). Thermal imaging of pigs and pig housing was used to assess the thermal comfort of animals under a given environmental condition and the collected information was used as a decision making tool for maximizing pig growth and profitability of the unit. Thermal imaging of the pigs was also used to study the metabolic activity of the animal at rest, during feeding and

after feeding (Kastberger and Stachil 2003). Thermal imaging of horses helped to locate the injuries in bones, joints, tendons, and muscles (Fuchs 2002). The hot spot in the skin surface showed the increased blood flow which was due to the inflammation or injury; and cold spots represented the decreased blood flow due to blood damage or blood clot. Hellebrand et al. (2003) used thermal imaging for health and fertility diagnostics of sucker cows. The cows with hot udders could be detected from the thermal images but determination of pregnancy using the changed skin temperature was not possible because the skin temperature was dominated by the ambient conditions.

Arenas et al. (2002) studied the feasibility of infrared thermal imaging system to diagnose mite infestation in Spanish ibex animals. They reported that thermal imaging system was sensitive to a maximum distance of 110 m from the animal and there was a significant correlation ($P<0.05$) between observation distance and positive diagnosis. Thermography had been used to measure the body and wing temperatures of flying bats (Lancaster et al. 1997). The average body temperature of bats were 38.0°, 38.5, 38.0°C at prior to flight, after 950 s of flight, and after 1890 s of flight, respectively. The mean temperature of the bats wings was always 1.8°C above the ambient temperature, and the temperatures of forearm muscle mass and trailing edge of wings were 34 and 24°C, respectively.

2.5 Applications in the Grain Handling Industry

Manickavasagan (2007) studied the potential applications of a thermal imaging in various grain handling operations like wheat class identification, detection of insect infestation, detection of a hot spot in a stored grain silo and, to observe the non-uniform

heating pattern during microwave heating of cereals and oilseeds. Wheat, barley and canola were dried using a pilot scale microwave drier for 28 and 56 s at five different power levels and thermal images were taken by a thermal camera. It had been observed that that the difference between the maximum and minimum surface temperatures of wheat, barley and canola were 62.9 to 69.5°C, 64.3 to 75.6°C and 39.5 to 59.2°C respectively, when the grains were exposed to 500W power level for 56 s.

Thermal images of a grain silo filled with wheat were taken and found that thermal imaging system can only detect hotspots which were located at 0.3m from the silo walls. Environmental conditions like the wind and cold weather largely affected the detection accuracy of the thermal imaging system (Manickavasagan 2007). Quadratic discriminant analysis (QDA) classification models were developed using the thermal images taken from the bulk wheat samples for identification of western Canadian wheat classes and yielded the accuracies of 76, 87, 79, and 95% in bootstrapping and 64, 87, 77, 91% in leave-one-out validation techniques for 8 classes mixed, 4 red classes mixed, 4 white classes mixed and pair-wise comparison, respectively (Manickavasagan 2007).

Internal infestation of *Cryptolestes ferrugineus* in wheat kernels was detected using the thermal imaging technique and the classification accuracies of the linear discriminate analysis, quadratic discriminant analysis models developed using the temperature data were 76.6, 83.5% for infested kernels and 83.0, 77.7% for healthy kernels, respectively.

Vadivambal et al. (2007) had studied temperature distribution of microwave-heated grains using the thermal imaging system and reported that the average temperature of rye grains with a moisture content of 14% after 28s exposure times for 0, 200, 300,

400, 500 W power levels were 27.6, 49.2, 65.1, 59.0, and 85.4°C, respectively and the for oats grains with the same moisture content , the mean temperature of grains at the same conditions were 27.2, 33.1, 35.5, 46.6, and 51.4°C, respectively. They also found cold and hot regions in the same sample and the temperature differences between these regions were 23 to 63°C and 7 to 25°C for rye and oats, respectively.

2.6 Fungal Infection in Stored Grain

Fungi represent a very large, diverse group of heterotrophic organisms which generally have a cell wall and are considered as a kingdom. In Canada, the most common cause for grain spoilage during storage is the growth of fungi on the grain (Muir and White 2001). On the basis of their behavior, grain fungi are divided into two groups: field fungi and storage fungi. The field fungi invade kernels before harvest, while the plants grow in the field, or after the grain is cut and swathed but before it is threshed. The major field fungi that attack the cereal grains are species of *Alternria*, *Cladosporium*, and *Fusarium*. Field fungi may affect the appearance and quality of the grains; however grain can be disinfected during drying operation before storage. Storage fungi invade the kernels once the grains are transferred into storage and these can spoil the whole grain mass under favorable conditions. The storage fungi include about a dozen species of *Aspergillus* and several species of *Penicillium* (Christensen and Kaufmann 1969). The *Aspergillus* spp. can grow from 13% and 8.5% m.c. in wheat and canola, respectively. *Penicillium* spp. requires high moisture content (17% for wheat and 11% for Canola). The major losses caused by fungi in stored grain are: (i) decrease in germinability; (ii) seed discoloration; (iii) heating and mustiness; (iv) changes in grain chemical

components; (v) loss in dry matter content; and (vi) production of mycotoxins. Detection of storage fungi in early stages is very important to reduce the quality and quantity losses of grain.

2.7 Fungal Detection Methods

2.7.1 Microscopic and biochemical methods

Generally, microbial culture methods like plate agar methods are used to detect fungal infection in stored cereal grains. These methods determine the relative amount of various fungal species present in the grain mass (Lacey et al. 1980). These techniques require a long incubation period and can be used to determine the only culturable fungi. Williams (1989) used a microscopic method for direct observation and quantification of fungal mycelium and reported that this method was a time consuming process and not suitable for rapid detection. Measurement of degradation of grain chemical components was used to determine the total colony forming units and time of microscopic inspection (Anderson 1970). The changes in α- and β-amylases and reducing sugar content of grain at 25°C and 0.95 water activity was used to access the fungal infection.

The biochemical changes induced by fungal growth on grains can be used to detect fungal infection in stored grain. Chitin is the main component of fungal cell walls, and the fungal invasion in corn and soybean seeds were detected by chitin measurement (Donald and Mirocha 1977). The hydrolysis of chitin to glucosamine can be measured by colorimetric methods (Jarvis et al. 1984, Ride and Drysdale, 1972). The high performance liquid chromatography (HPLC) method was used to measure the

glucosamine level which differs between the fungal species by which the fungal infection was detected (Lin and Cousin, 1985). But, all these methods need a long observation time and hence rapid detection of fungi is not possible.

2.7.2 Detection by measuring volatiles

Spoiled grain often develops off-odors in storage, and 3-methyl-1-butanol, 1-octane-3-ol and 3-octanol are the most common volatiles produced by the storage fungi (Abramson et al. 1980). These volatiles can be detected by various techniques such as, gas chromatography, mass spectrometry, and sensory analysis (Schnurer et al. 1999; Smith et al. 1994; Keshri et al. 1998). These volatiles can also be measured by an "electronic nose" system (Keshri et al. 1998). The electrical signals produced by the sensors in the "electronic nose" were processed with multivariate statistical classifiers, and healthy, *Eurotium(Aspergillus)* sp. infected, and *Penicillium* sp. infected grain samples were differentiated using volatile patterns produced by fungi. Keshri and Magan (2000) also used the electronic nose system to detect and differentiate mycotoxigenic and non-mycotoxigenic fungi infection in cereal grains. The *F. moniliforme* and *F. proliferatum* fungal cultures inoculated wheat grains at 25°C and 0.95 water activity. The volatiles produced in the head space of the healthy, mycotoxinic and non-mycotoxinic fungi cultures were observed by the "electronic nose" and β-D-glucosidase and N-acetyl-β-D-glucosiminidase increased significantly in non-mycotoxigenic fungal-infected samples as compared to mycotoxigenic samples. The chemical ionization of volatile compounds was measured by a Selected Ion Flow Tube-Mass Spectrometry (SIFT-MS), and the volatile pattern produced by *Aspergillus flavus*, *Aspergillus fumigatus*, *Candida*

albicans, *Mucor racemosus*, *Fusarium solani*, and *Cryptococcus neoformans*-infected samples were detected (Scotter et al. 2005).

2.7.3 Imaging techniques

Pearson et al. (2001) used near-infrared transmittance (NIRT) and near-infrared reflectance (NIRR) spectroscopy methods for detecting aflatoxin-infected corn kernels. They used NIR transmittance and reflectance spectra values for developing partial least square (PLS) regression calibration models. Though, this model could not predict the concentration of the aflatoxin accurately, more than 95% of the corn kernels were correctly classified into either a low level (<10 ppb) or high level (>100 ppb) of aflatoxin infection. Dowell et al. (2002) also used the NIRT and NIRR spectroscopy method for detecting the fumonosine produced by *Fusarium vericillioides*, but they also classified the kernels with >100 ppm and <10 ppm into fumonisin positive or negative kernels, respectively.

Pearson et al. (2004) developed a high-speed dual-wavelength sorter for removing the aflatoxin and fumonisin contaminated yellow corn kernels. They found that single kernel NIR reflectance spectra at 750 and 1200 nm classified >95% of the corn kernels into aflatoxin contaminated or uncontaminated. This sorter reduced 81% of aflatoxin and 85% of fumonisin from their initial levels.

Pearson and Wicklow (2006) compared the single-kernel reflectance spectra (550 to 1700 nm), visible color reflectance images, x-ray images, multi-spectral transmittance images (visible and NIR), and physical properties (mass, length, width, thickness, and cross-sectional area) for detection of fungal infection in corn kernels. They found that the

NIR reflectance spectral bands at 715 nm and 965 nm could correctly identify 98.1% and 96.6% of healthy and fungal-infected kernels, respectively. The histogram features of the visible transmittance images correctly identified 96.2% uninfected and 91.9% fungal infected kernels.

A semi-automated wheat scab inspection system was developed based on the NIR reflectance of single wheat kernels and used to classify the wheat kernels into scab-damaged, mold damaged, and sound kernels (Delwiche 2003). The reflectance spectra of each kernel in 940 - 1700 nm range at every 6 nm interval was collected by using NIR diode array spectrometer and linear discriminant and non parametric classification models were developed. The reflectance spectra at 1200 nm wavelength gave 95% classification accuracies for healthy and scab-damaged kernels. But, classification of scab-damaged, mold damaged, and sound kernels were not possible using this system.

Singh et al. (2007) used near-infrared hyperspectral imaging system for identification of fungal infection in wheat kernels. Wheat kernels infected by *A. glaucus*, *A. niger* and *Penicillium spp.* were scanned along with sound kernels at a wavelength range of 1000 to 1600 nm, and they reported that the wavelengths at 1284.2, 1315.8, and 1347.4 nm gave highest factor loading in principal component analysis. The linear discriminant classifier developed from the hyperspectral data had classification accuracies of 97.8% for fungal-infected kernels and 95.0% for healthy kernels, and the quadratic and Mahalanobis discriminant classifiers had 93.3 and 96.1% classification accuracies for fungal infected kernels. But the all three four-way classifiers yielded

comparatively low classification accuracies for both sound and infected kernels (41.7-95% in linear, 58.3-95.0% in quadratic, and 30.0-93.3% in Mahalanobis classifiers).

2.8 Summary

There is a scope for using infrared thermal imaging system to identify the fungal infection in wheat grains. Fungal infection in the stored grains creates biochemical changes and these changes may cause some differences in temperature profile during heating and cooling of grains. A thermal imaging system was used to classify the Western Canadian wheat classes based on the temperature profile changes during heating (Manickavasagan 2007). The statistical classifiers produced good results in identifying wheat classes and insect infestation. As fungi consume grain chemical components for their growth, there may be some differences in grain components between low and highly infected grains. There have been only a limited number of studies done for the fungal detection in grains using machine vision techniques. Thus, there is a need to assess the ability of thermal imaging system to detect fungi in stored wheat.

Chapter 3

MATERIALS AND METHODS

3.1 Grain Sample Preparation

Fungal-infected wheat samples were prepared at the Cereal Research Centre, Agriculture and Agri-Food Canada, Winnipeg, MB. Three sp. of fungi, *Aspergillus glaucus*, *Aspergillus niger*, and *Penicillium spp.*, were cultured on old stored wheat kernels placed on filter papers saturated with 7.5 mL aqueous NaCl solution in petri dishes. Pure fungal lines from these infected kernels were collected after 7 days and placed on potato dextrose agar (PDA) medium for 1 wk at 30°C. Then this agar medium with mold were transferred to a plastic spray bottle containing 200 mL sterilized water with one drop of Polysorbate 20 (commercially known as Tween 20) and shaken for 1-2 min to prepare the fungal solution.

About 20 kg of Canada Western Red Spring (CWRS) wheat (cv. 'AC Barrie') conditioned to a moisture content of 19% (wet basis) was soaked in to 1% sodium hypochlorite for 2 min for surface sterilization. Then, the wheat grains were rinsed by sterilized water and kept on the paper towels for 2 h. A 2 kg moistened wheat sample per

fungus sp. was taken and placed in a large plastic tub in few kernel deep layers and misted with fungal solution in fume hood. This setup was covered with a loose plastic bag, and the bag was kept at 30°C. *Aspergillus glaucus* and *Aspergillus niger* samples were collected at following 4 infection levels: (i) 1 wk after fungal inoculation; (ii) 3 wk after inoculation; (iii) 5 wk after inoculation; (iv) 8 wk after inoculation by shaking the sample fume hood for 1 min in four plastic bags sequentially and pouring them into a fifth plastic bag. Then the sample collected in the fifth plastic bag was stored at -10° C in a freezer. *Penicillium* spp. infected sample was collected 8 wk after inoculation using the above sampling procedure and stored at -10°C. All the samples were taken out from the freezer and dried to 14% m.c. (wet basis). Then samples were kept at the room temperature for 5 h. The control sample also conditioned to the 14% m.c. (wet basis) by a grain conditioner and kept at room temperature.

3.2 Image Acquisition and Analysis

3.2.1 Hardware

The experimental setup used for this study is given in Figure 3.1. It had 2 major components namely: (i) thermal camera unit and (ii) heating unit.

An un-cooled focal planar array type infrared thermal camera (Model: THERMOCAM™ SC500 of FLIR systems, Burlington, ON) with a resolution of 320 × 240 pixels and a spectral range of 7.5 to 13.0 μm was used for the image acquisition. Thermal sensitivity of the camera was 0.07°C at 30°C and the instantaneous field of view

was 1.3 mrad with the built-in lens focus of 24° × 18°. While taking the thermal images, the emissivity (ε) of the grain was set at 0.98 and the ambient temperature and relative humidity were measured using a commercial hygrometer and inputted to the system. Thermal camera was fixed at a height of 40cm above the grain. Twenty-five grams of grain sample were taken and spread in a single layer of 10 × 10 cm on the base of the camera stand (Model: Copymate II copystand 900-20 SC, Bencher Inc., Antioch, IL). The surface temperature of the base was maintained at a temperature of 30±0.05°C before placing the grain sample.

A plate type heater with a temperature control mechanism was used for heating the grain samples. A steel plate (175 × 175 × 2mm) was heated by a heat tape and a thermocouple was used to measure the temperature of the bottom surface of the steel plate. A proportional with integral and derivative (PID) temperature controlling unit was used to control the plate temperature and this plate was fixed with a stand using a hinge joint which provided a swing motion to the plate heater. The temperature of the plate heater was set at 90°C and placed 10 mm above the grain sample. Wheat samples were heated for 180 s, after that plate heater was swung away from the samples, and samples were allowed to cool for the next 30 s. Three thermal images: 1. before heating, 2. after heating (for 180 s), and 3. after cooling (for 30 s) were taken for each sample. One hundred replications were done for each sample. A total of 3000 (3 imaging periods × 100 replications per treatment × 10 treatments) images were acquired in this study.

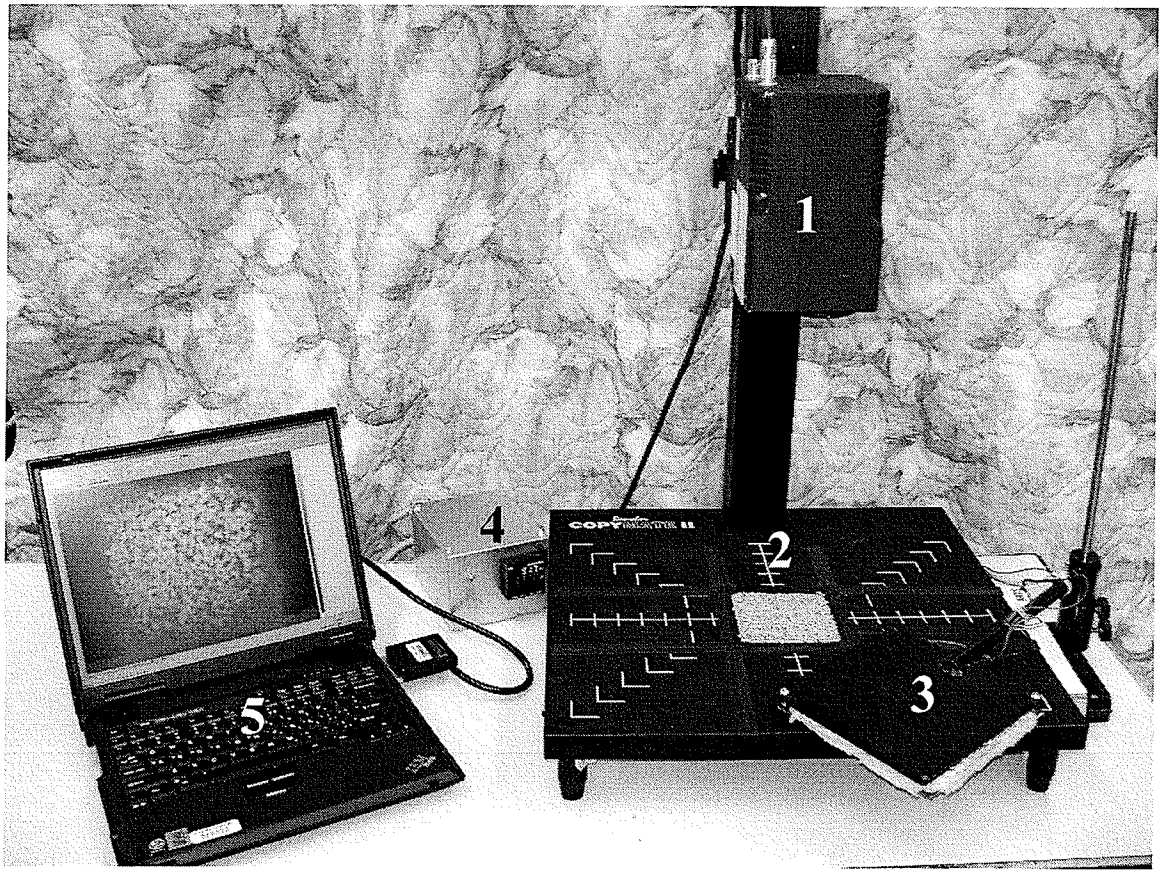

Figure 3.1 Experimental setup of the near-infrared thermal imaging system to identify the fungal infection in wheat

1. Thermal camera 2. Wheat sample 3. Plate heater 4. PID temperature controller 5. Data acquisition system

3.2.2 Software

ThermaCAM Researcher 2001 software (FLIR systems, Berlington, Ontario, Canada) was used to acquire the images. The actual size of the thermal image was 320×240 pixels, and the sample occupied 150×150 pixels only. An Algorithm was developed in Matlab (Version 7.1b2007, The Mathworks Inc., Natick, MA) to segment the portion occupied by the grain and extract the temperature data (150×150 =22500 temperature values) for each image. From each image, mean, maximum, minimum, median, mode and standard deviation of the surface temperatures of the grain were extracted using this algorithm.

3.3 Classification Model Development

Linear dicriminant analysis (LDA) and quadratic discriminant analysis (QDA) models were used to classify the fungal-infected and healthy samples. The temperature features data used for the classification model development are given in Table 3.1. The PROC DISCRIM procedure in SAS (version 9.1.3, SAS Institute Inc., Cary, N.C.) was used for developing classification models. It calculates the generalized squared distance of group means and based on this generalized squared distance of a group mean each observation (response variable) is assigned a probability of belonging to a given group. In linear discriminant function, the classification is based on the pooled covariance matrix and in quadratic discriminant function, classification is based on an individual within-group covariance matrix. For validating the developed discriminant functions, two types of validation techniques: leave-one-out and bootstrap were used.

Table 3.1 Derived temperature features used for the classification model.

Name	Description
ΔT_{Hmean}	(mean surface temperature of grain bulk after heating) - (mean surface temperature of grain bulk before heating)
ΔT_{Hmax}	(maximum surface temperature of grain bulk after heating) - (maximum surface temperature of grain bulk before heating)
ΔT_{Hmin}	(minimum surface temperature of grain bulk after heating) - (minimum surface temperature of grain bulk before heating)
$\Delta T_{Hmedian}$	(median of surface temperatures of grain bulk after heating) - (median of surface temperatures of grain bulk before heating)
ΔT_{Hmode}	(mode of surface temperatures of grain bulk after heating) - (mode of surface temperatures of grain bulk before heating)
ΔT_{Hstd}	(standard deviation of the surface temperatures of grain bulk after heating) - (standard deviations of the surface temperatures of grain bulk before heating)
ΔT_{Cmean}	(mean surface temperature of grain bulk after heating) - (mean surface temperature of grain bulk after cooling)
ΔT_{Cmax}	(maximum surface temperature of grain bulk after heating) - (maximum surface temperature of grain bulk after cooling)
ΔT_{Cmin}	(minimum surface temperature of grain bulk after heating) - (minimum surface temperature of grain bulk after cooling)
$\Delta T_{Cmedian}$	(median of surface temperatures of grain bulk after heating) - (median of surface temperatures of grain bulk after cooling)
ΔT_{Cmode}	(mode of surface temperatures of grain bulk after heating) - (mode of surface temperatures of grain bulk after cooling)
ΔT_{Cstd}	(standard deviation of the surface temperatures of grain bulk after heating) - (standard deviation of the surface temperatures of grain bulk after cooling)

In the leave-one-out method, one observation is randomly removed from the given dataset with n observations. The classification model is developed using the remaining (n-1) observations, which is called as training dataset. Then the removed single observation is used as a test or validation dataset. This data separation process is continued to develop n training and validation datasets. Models are developed and validated for each pair of training and validation datasets. The performance of the model (classification accuracy) on n number of validation datasets was determined and average classification accuracy was calculated.

To minimize the sampling error and increase the robustness of the classification model, the bootstrap validation method was used. In this study, 1000 bootstrap samples, each with 100 observations were created. In this method, n observations with replacements were randomly drawn from the original data set to create a single bootstrap sample. The classification model developed from each bootstrap sample was validated against the original dataset and relevant estimates of prediction errors were determined. Then average estimates of prediction errors were calculated for total N bootstrap samples (in this study, 1000 bootstrap samples).

In this study, four types of discriminant analyses were performed using both LDA and QDA models: (i) 10-way classification (healthy and 9 fungal infected samples mixed); (ii) 3-way classification (healthy and 2 species of fungal infected samples); (iii) two types of pair-wise comparison (healthy versus infected, and healthy versus each fungal species at each infection level);and (iv) two types of comparisons based on infection levels (healthy versus same level of fungal infection samples mixed, and healthy versus low and highly infected samples).

Chapter 4

RESULTS AND DISCUSSION

4.1 Temperature Changes during Heating

PROC MEANS procedure in SAS (version 9.1.3, SAS Institute Inc., Cary, N.C) was used for calculating the mean and standard deviation of the temperature features derived from the thermal data. Statistics of derived temperature features during heating are given in Table 4.1. Temperature profiles of different species of fungal-infected wheat samples after heating for 180 s were significantly different (α=0.05) from each other. Temperature profiles of the fungal-infected samples were also significantly (α=0.05) different from the healthy wheat samples. The surface temperature rise of *A. glaucus* infected samples were gradually increased from 12.68 to 13.81°C from 1 wk to 8 wk of infection, and in *A. niger* infected samples also behaved similarly (from 12.38 to 13.68°C). PROC GLM procedure was used for least squared means test and temperature features were grouped by Scheffe's test. There was some overlap between the fungal infected samples. For example, mean temperature rises for 1 wk after *A. glaucus* and *A. niger* infection were not significantly different. Low level fungal-infected samples tend

to fall in the same group and high-level infected samples fall in different groups. Scheffe's test results also proved that, mean surface temperature rise of healthy grains were significantly lower from the fungal infected grains. The temperature rise of healthy grains was distinctive and did not overlap with any of the fungal-infected samples by all temperature features except ΔT_{Hstd}. Results of the t statistics showed that there were many overlaps in the case of ΔT_{Hstd}, and this resulted in a formation of the least number of clusters. All three central tendancy factors (mean, median, and mode) followed the same trend: all low infection samples grouped in one class and high infection samples tend to fall in another class.

4.2 Temperature Changes during Cooling

Mean surface temperature of the healthy wheat grains dropped about 2.69°C after 30 s cooling. Statistics of the derived temperature features after cooling are given in Table 4.2. For *A. glaucus*-infected samples, temperature drop after 30 s cooling were 2.88, 3.01, 3.46 and 3.65°C for 1 wk, 3 wk, 5 wk and 8 wk after infection, respectively. For *A. niger*-infected samples, the temperature drop of 2.81, 3.03, 3.39, and 3.54°C were recorded for 1 wk, 3 wk, 5 wk and 8 wk after infection, and for 8 wk *Penicillium spp.* infected sample temperature drop was 3.47°C. Comparison of sample means using Scheffe's test showed that, the mean temperature drop of healthy grains was significantly lower from that of fungal infected samples, and there were many overlaps observed between the fungal-infected samples. All temperature features showed the same trend: all low level fungal infected samples (1 and 3 wk of infection) fall in the same group and highly infected samples (5 and 8 wk of infection) tend to fall in another group. In temperature drop analysis, ΔT_{Cmean} formed maximum number of clusters and ΔT_{Cmin}, ΔT_{Cmode}, and, ΔT_{Cstd} formed minimum number of clusters by t statistics. In all temperature features, the number of clusters formed by the temperature rise data was more than that of temperature drop data.

Table 4.1 Temperature features (°C) for wheat at different fungal infection levels after heating for 180 s.

Sample	ΔT_{Hmean}	ΔT_{Hmax}	ΔT_{Hmin}	$\Delta T_{Hmedian}$	ΔT_{Hmode}	ΔT_{Hstd}
Healthy	11.40^{f}*±0.84**	12.17^{e} ±1.40	8.66^{e}±0.87	11.56^{f}±0.79	12.05^{e}±0.88	0.64^{d}±0.19
A. glaucus 1 wk	12.68^{de}±0.94	13.81^{d}±1.03	10.00^{bc}±0.78	12.72^{ed}±0.96	12.70^{cd}±1.11	0.62^{de}±0.16
A. niger 1 wk	12.38^{e}±0.63	13.56^{d}±0.77	9.56^{b}±0.66	12.41^{e}±0.66	12.35^{de}±0.89	0.65^{d}±0.16
A. glaucus 3 wk	13.07^{cd}±0.68	14.01^{d}±0.81	10.36^{ab}±0.69	13.11^{cd}±0.69	12.96^{bc}±0.73	0.57^{de}±0.18
A. niger 3 wk	13.24^{c}±0.73	13.95^{d}±0.85	10.56^{a}±0.76	13.19^{c}±0.74	13.25^{ab}±0.80	0.52^{e}±0.16
A. glaucus 5 wk	13.26^{c}±0.56	15.77^{c}±1.05	9.92^{bcd}±0.75	13.30^{bc}±0.55	13.11^{bc}±0.59	0.89^{b}±0.19
A. niger 5 wk	13.26^{c}±0.53	15.77^{c}±1.02	9.92^{bcd}±0.67	13.30^{bc}±0.53	12.95^{bc}±0.63	0.89^{b}±0.17
A. glaucus 8 wk	13.81^{bc}±0.64	16.56^{c}±1.04	9.86^{cd}±0.74	13.76^{bc}±0.65	13.42^{abc}±0.67	1.09^{b}±0.17
A. niger 8 wk	13.67^{ab}±0.73	16.44^{ab}±1.19	9.81^{cd}±0.76	13.61^{ab}±0.73	13.22^{ab}±0.77	1.05^{a}±0.19
Penicillium 8 wk	13.38^{bc}±0.59	16.15^{abc}±1.33	9.98^{bcd}±0.83	13.37^{abc}±0.61	13.17^{ab}±0.71	0.76^{c}±0.15

* values with same letters in a column are not significantly differ (α = 0.05) by t test, ** standard deviation (n=100)

Table 4.2 Temperature features (°C) for wheat at different fungal infection levels after cooling for 30 s.

Sample	ΔT_{Cmean}	ΔT_{Cmax}	ΔT_{Cmin}	$\Delta T_{Cmedian}$	ΔT_{Cmode}	ΔT_{Cstd}
Healthy	2.69[e]*±0.22**	3.63 [d]±0.71	1.67 [bc]±0.35	2.70 [d]±0.22	2.72 [bc]±0.43	0.31 [c]±0.11
A. glaucus 1 wk	2.88 [cd]±0.24	4.18 [c]±0.46	1.65 [bc]±0.25	2.85 [cd]±0.24	2.66 [c]±0.44	0.39 [b]±0.06
A. niger 1 wk	2.81 [de]±0.30	4.12 [c]±0.48	1.55 [c]±0.38	2.77 [d]±0.31	2.50 [c]±0.56	0.40 [b]±0.08
A. glaucus 3 wk	3.01 [c]±0.45	4.40 [c]±0.64	1.63 [bc]±0.27	2.97 [c]±0.46	2.67 [c]±0.58	0.40 [b]±0.07
A. niger 3 wk	3.03 [c]±0.21	4.40 [c]±0.42	1.66 [bc]±0.24	2.99 [c]±0.20	2.78 [bc]±0.41	0.41 [b]±0.06
A. glaucus 5 wk	3.46 [b]±0.19	5.51 [b]±0.65	1.65 [bc]±0.31	3.40 [ab]±0.19	3.19 [a]±0.47	0.53 [a]±0.04
A. niger 5 wk	3.39 [b]±0.25	5.49 [b]±0.65	1.57 [bc]±0.35	3.31 [b]±0.25	3.11 [a]±0.48	0.56 [a]±0.06
A. glaucus 8 wk	3.65 [a]±0.31	5.69 [b]±0.85	1.89 [a]±0.34	3.54 [a]±0.31	3.10 [a]±0.63	0.54 [a]±0.8
A. niger 8 wk	3.54 [ab]±0.29	5.73 [b]±0.86	1.74 [ab]±0.36	3.41 [ab]±0.26	2.99 [ab]±0.50	0.56 [a]±0.08
Penicillium 8 wk	3.47 [b]±0.21	6.20 [a]±1.01	1.74 [ab]±0.29	3.40 [ab]±0.21	3.20 [a]±0.43	0.55 [a]±0.05

* values with same letters in a column are not significantly differ (α = 0.05) by t test, ** standard deviation (n=100)

4.3 Relationship between Temperature Rise and Grain Chemical Component Changes

Growth of fungi in grains changes the chemical components of the wheat grain in the following manner: (i) increase the free fatty acids and reducing sugars; (ii) create protein changes including enzyme activity changes and (iii) production of fungal constituents like mycotoxins (Tipples 1995). Farag et al. (1985) observed 0.5% increase in the lipid content due to the fungal infection in wheat grains, and the reducing sugar content also increased 3 to 6 times. Wheat kernels infected with *Aspergillus* spp. had the highest amount of reducing sugars and it was about 3 times higher than that of other fungal-infected samples. The fungi utilize the grain chemical constituents for their growth. Farag et al. (1985) measured the chemical composition of the storage fungal species on dry basis and reported that nearly 20% of fungal weight contains protein. The protein content of the mold-damaged wheat samples may increase due to the respiratory loss of carbohydrates (Pomeranz 1992) and Farag et al. (1985) found that the protein content of fungal infected wheat samples increased about 3.77 to 9.35% depending on fungal genus. The growth of fungal activity of stored grains was correlated with an increase in free fatty acids, which is mainly due to the fungal lipase activities. These biochemical changes induced by the fungal growth may develop some changes in the temperature pattern of the grains during heating and cooling. Manickavasagan (2007) reported that the changes in chemical composition of wheat caused some changes in the grain's temperature profile and the grain quality parameters had correlation coefficients

of 0.17 to 0.65 with the temperature rise. He also reported protein content of wheat had the highest correlation with the rate of heating and cooling.

4.4 Relationship between Temperature Rise and Specific Heat of Grain

Specific heat or specific heat capacity is defined as the amount of heat energy required per unit mass to increase the temperature by 1°C. The relationship between temperature rise and heat can be easily defined by the following equation for biological and non-biological materials:

$$Q = cm\Delta T \tag{4.1}$$

Where:

Q = heat added (J)

c = specific heat ($Jg^{-1}K^{-1}$)

m = mass of the material (g), and

ΔT = change in temperature (K).

From the Eqn 4.1, we can derive the relationship between the temperature change and the specific heat, where change in temperature is inversely proportional to the specific heat of the material.

For biological materials, the following formula can be used to determine the specific heat of the materials with known chemical components (Singh and Heldmen, 1993).

$$c = 1.424m_c + 1.549m_p + 1.675m_f + 0.837m_a + 4.187m_m \tag{4.2}$$

Where:

c = specific heat of the sample ($Jg^{-1}K^{-1}$)

m_c = mass fraction of carbohydrate

m_p = mass fraction of protein

m_f = mass fraction of fat

m_a = mass fraction of ash, and

m_m = mass fraction of moisture content of the sample.

Farag et al. (1985) measured the chemical composition of healthy and various fungal infected wheat samples and the specific heat of samples calculated from these values were in the range of 1.96, and 1.94 for healthy and fungal-infected samples, respectively, at 14% moisture content. The temperature rise after 180 s heating of healthy and fungal-infected samples compared with the specific heat values, and the temperature rise was found inversely proportional to the specific heat values.

4.5 Classification using LDA

PROC DISCRIM function in SAS (version 9.1.3, SAS Institute Inc., Cary, N.C) was used to develop linear discriminant analysis (LDA) models for classification of fungal infection in wheat samples. All 12 derived temperature features (6 from temperature rise data and 6 from temperature drop data) were used as input values for developing the classification model. The linear discriminate function developed from the temperature features was performed with two validation techniques such as: leave-one-out method and bootstrapping method to increase the robustness of the classification model.

4.5.1 10-way classification

Classification accuracies of leave-one-out and bootstrap methods of LDA models are shown in Figure 4.1. For all 10 samples (healthy, 4 stages of *A. glaucus* infected, 4 stages of *A. niger*- infected and 1 *Penicillium*-infected) mixed together, the classification accuracies of healthy samples were 71.0 and 71.9% using leave-one-out and bootstrap methods, respectively. In *A. glaucus*-infected samples, classification accuracies ranged from 25.0 to 50.0% using the leave-one-out method and from 29.0 to 58.7% using bootstrapping methods. Classification accuracies of *A. niger*-infected samples were 36.0 to 54.0% and 44.0 to 59.0% using leave-one-out and bootstrapping methods, respectively. For the *Penicillium* spp.-infected sample, classification accuracy using leave-one-out and bootstrapping methods were 68.0 and 69.2%, respectively. For all samples, classification accuracies using bootstrapping method were higher than that of using leave-one-out method. The temperature profile of the healthy grain samples was different from fungal infected samples after heating, and it yielded the highest classification accuracy. Most of the time, healthy samples were misclassified with the 1 wk fungal-infected samples. In fungal infected samples, one fungal infected sample was misclassified as another species with the same level of infection, for instance, most of the 1 wk *A. glaucus* samples were misclassified with the 1 wk *A. niger*-infected samples. In fungal-infected samples, 8 wk *Penicillium* spp.-infected sample had higher classification accuracy using both validation techniques, and most of the misclassification happened with 8 week *A. glaucus* and *A. niger*-infected samples. The grain samples used for this study are shown in Figure 4.2. Fungal infection in wheat can be visibly distinguable only from 5 wk or longer infection levels. Fungal growth in cereal grains changes the chemical composition of grains and

wheat grain supports the fungal growth more than other major cereal grains. In wheat, fungal growth reduces the lipid and starch contents (Madhyastha et al., 1993). So, the chemical composition difference between healthy and fungal-infected grains was more

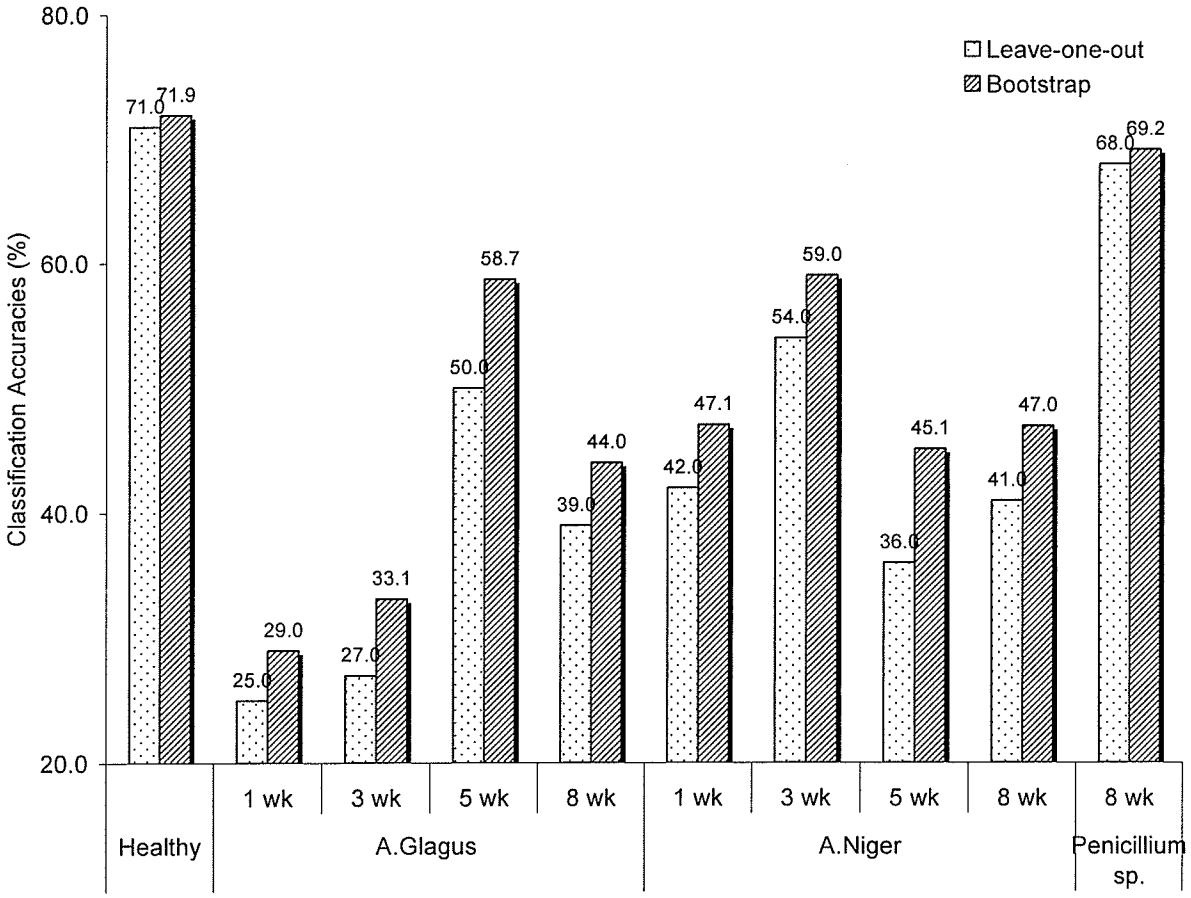

and there may be no significant difference in chemical composition between the grains infected by various fungal species.

Figure 4.1 Classification accuracies of a 10-way LDA model for healthy and fungal-infected wheat samples at different levels of fungal infection using leave-one-out and bootstrapping validation techniques.

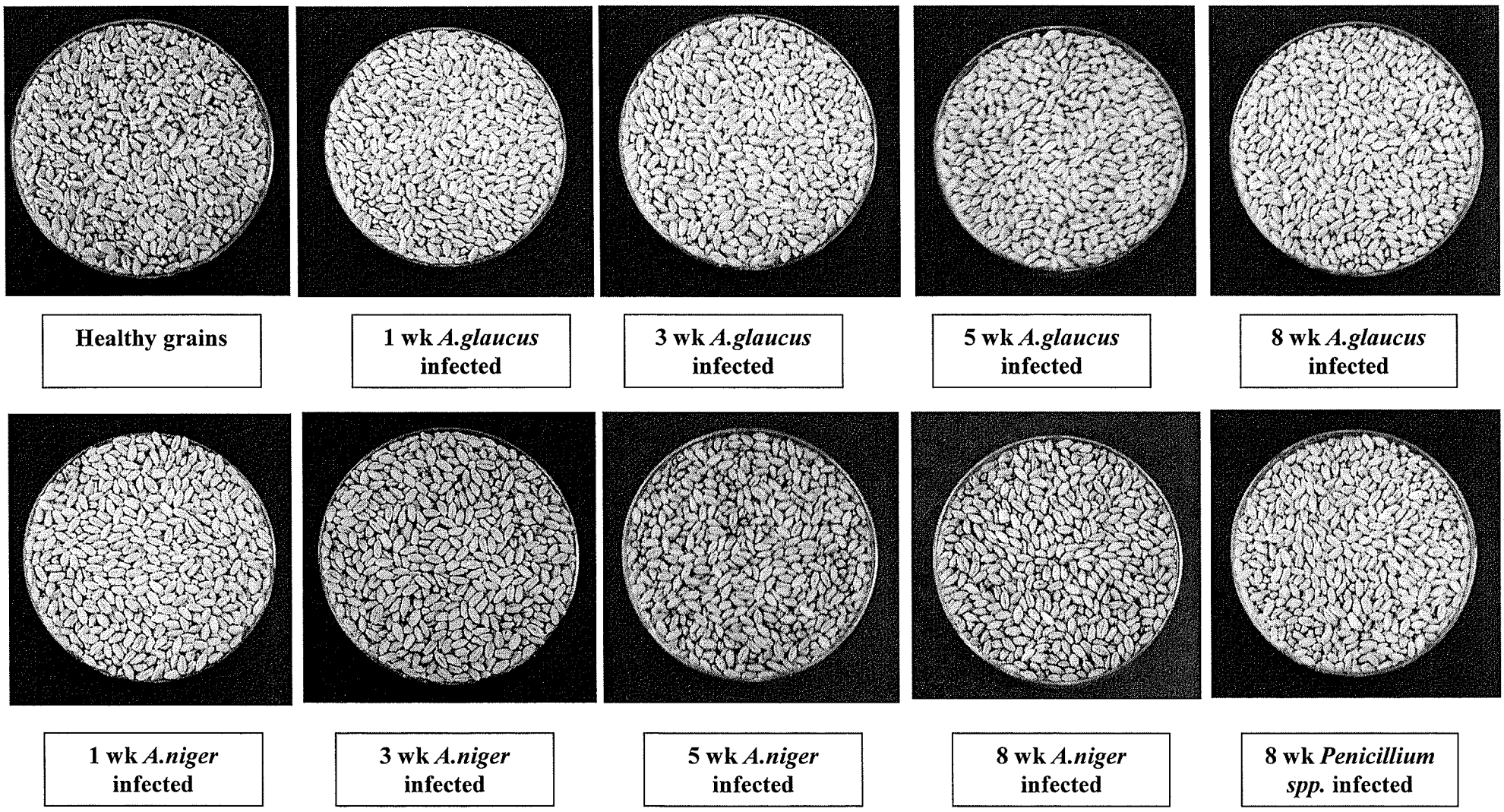

Figure 4.2 Healthy and fungal-infected wheat samples at different levels of fungal infection

4.5.2 3-way classification

In 3-way classification LDA model, fungal-infected samples at the same infection level were compared with healthy samples. Classification accuracies of the 3-way LDA model using leave-one-out and bootstrapping validation methods are given in Figure 4.2. Classification accuracies for 1wk of *A. glaucus* and *A. niger*-infected samples were 61.0 and 46.0%, 64.8 and 57.0% using leave-one-out and bootstrapping methods, respectively, and for healthy samples the accuracies were 72.0 and 78.9%.

Healthy wheat samples had a maximum accuracy of 99.0% using the leave-one-out method and 100.0% using bootstrapping method for 5 wk infection samples. For *A. glaucus* infection samples, classification accuracies ranged between 46.0 and 61.0% using the leave-one-out method, 55.1 and 66.8% in the bootstrapping method, respectively. For *A. niger*-infected samples, the classification accuracies were in the range of 46.0 to 62.0%, and 52.1 to 65.1% using the leave-one-out, and bootstrapping methods, respectively. For *Penicillium spp.* infected samples, classification accuracies were 71.0 and 74.1% using the leave-one-out and bootstrapping validation techniques. In the 3-way classification model most of the misclassifications occurred between the fungal species, and misclassification between fungal and healthy samples were rare (<4.0%) beyond 3 wk of infection.

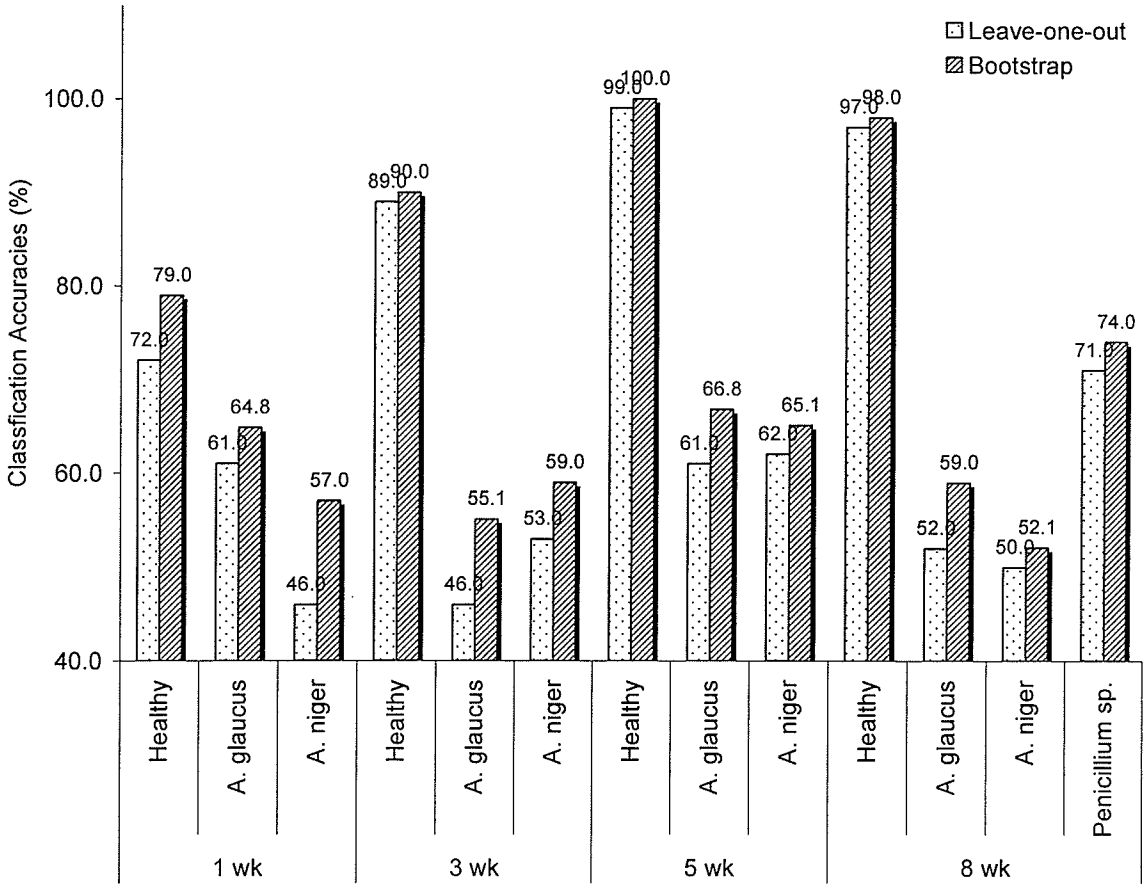

Figure 4.3 Classification accuracies of a 3-way LDA classification model for healthy and fungal-infected wheat samples at different levels of fungal infection using leave-one-out and bootstrapping validation techniques.

4.5.3 Pair-wise comparison

In pair-wise comparison, there were two types of analysis done in this study: (i) healthy versus infected at different infection levels and (ii) healthy versus particular species of fungal infection at different infection levels.

In healthy versus infected type of analysis, all the fungal-infected samples at same infection level were mixed together and compared with healthy samples. The classification accuracies of healthy and fungal-infected samples at 1 wk, 3 wk, 5 wk, and 8 wk after infection are given in Figure 4.3. For healthy samples, an accuracy of 95.5 and 93.1% using the leave-one-out and bootstrapping methods were achieved at 3 wk after infection, and 100.0% accuracy was obtained in both validation methods for 5 wk after infection samples. For fungal-infected samples after 3 wk or longer, classification accuracies were in the range of 93.0 to 99.3%, and 94.5 to 99.0% using the leave-one-out and bootstrapping validation techniques, respectively. Classification accuracies of 90.0 and 96.0% were obtained using leave-one-out and bootstrapping validation techniques in 3 wk infection samples.

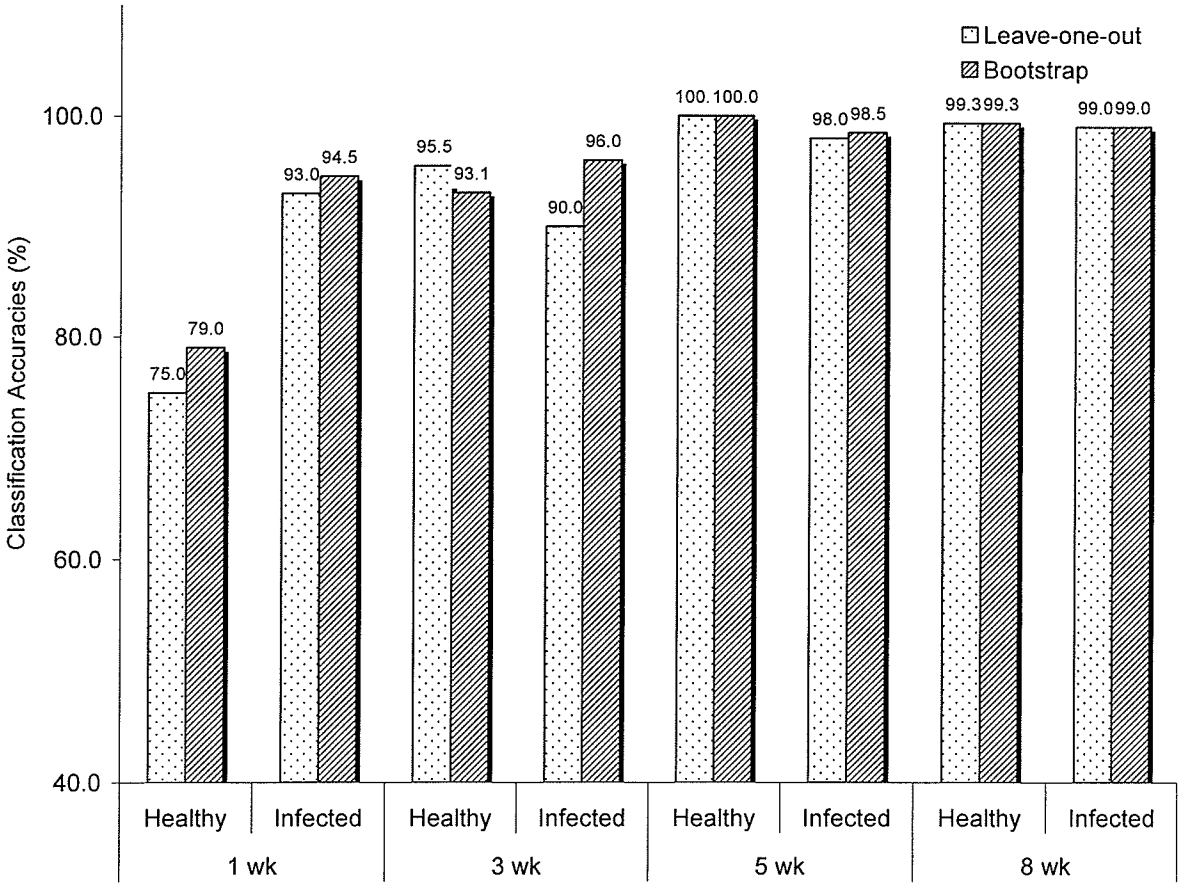

Figure 4.4 Classification accuracies of a pair-wise LDA classification model for healthy and fungal-infected wheat samples at different levels of fungal infection using leave-one-out and bootstrapping validation techniques.

In another type of linear discriminant analysis, healthy grain samples were compared with *A. glaucus*, *A. niger* and *Penicillium spp.*-infected samples at different infection levels. Classification accuracies of healthy and different fungal species at 4 different infection levels using the leave-one-out and bootstrapping validation methods are given in Tables 4.3 and 4.4. After 1 wk of infection, *A. glaucus* samples had a classification accuracy of 93.0% in both validation techniques, and *A. niger* samples had 90.0 and 91.0% of accuracy using leave-one-out and bootstrapping methods, respectively. But, the healthy samples had an average accuracy of 79.0% with both infected samples. While comparing 3 wk infection samples with healthy samples, only 5.0% of *A. glaucus* and 6.0% of *A. niger*-infected samples were misclassified as healthy samples using leave-one-out method, and 4.0 and 6.0% misclassification occurred using bootstrapping method. Beyond 5 wk of infection, an average of 99.0% classification accuracy was obtained for both species of fungal infection using both validation techniques. The 8 wk *Penicillium* spp.-infected sample had 98.0 and 100.0% classification accuracy using leave-one-out and bootstrapping methods. Singh et al. (2007) got 100.0, 95.0 and 88.3% classification accuracy for *Penicillum*, *A. niger* and *A. glaucus* infected wheat kernels in a pair-wise LDA model developed by near- infrared hyperspectral data. They also observed significant amount of misclassification between the fungal species in 4-way LDA classifiers.

Table 4.3 Pair-wise discrimination of fungal-infected wheat grains from healthy by linear discriminant analysis (LDA) using leave-one-out validation technique

Fungi	Classification accuracies at various infection periods (%)							
	1 wk		3 wk		5 wk		8 wk	
	A.glaucus	Healthy	*A.glaucus*	Healthy	*A.glaucus*	Healthy	*A.glaucus*	Healthy
A.glaucus	93.0	77.0	95.0	92.0	97.0	99.0	97.0	100.0
	A. niger	Healthy	*A. niger*	Healthy	*A. niger*	Healthy	*A. niger*	Healthy
A. niger	90.0	78.0	94.0	91.0	97.0	100.0	98.0	100.0
	Penicillium	Healthy	*Penicillium*	Healthy	*Penicillium*	Healthy	*Penicillium*	Healthy
Penicillium	-	-	-	-	-	-	98.0	100.0

Table 4.4 Pair-wise discrimination of fungal-infected wheat grains from healthy by linear discriminant analysis (LDA) using bootstrapping validation technique

Fungi	Classification accuracies at various infection periods (%)							
	1 wk		3 wk		5 wk		8 wk	
	A.glaucus	Healthy	*A.glaucus*	Healthy	*A.glaucus*	Healthy	*A.glaucus*	Healthy
A.glaucus	93.0	80.0	96.0	95.0	98.0	100.0	99.0	100.0
	A. niger	Healthy	*A. niger*	Healthy	*A. niger*	Healthy	*A. niger*	Healthy
A. niger	91.0	81.0	94.0	93.0	98.0	100.0	98.0	100.0
	Penicillium	Healthy	*Penicillium*	Healthy	*Penicillium*	Healthy	*Penicillium*	Healthy
Penicillium	-	-	-	-	-	-	100.0	100.0

4.5.4 Comparison based on infection levels

Classifications accuracies of the LDA model were improved and the different levels of infection were analyzed separately. In the 5-way classification, the same level of fungal-infected samples (both *A. glaucus* and *A. niger*-infected samples) was mixed together and made into one single sample. The four fungal infected samples (1 wk, 3 wk, 5 wk, 8 wk of infection samples) were analyzed with one healthy sample. Using the leave-one-out validation method, classification accuracies of healthy, 1 wk, 3 wk, 5 wk, and 8 wk infected samples were 73.0, 64.5, 74.0, 77.0, and 78.3%, respectively, and using the bootstrapping method the classification accuracies of the same samples were 74.0, 68.6, 75.0, 77.5, 79.6%, respectively (Figure 4.4). Classification accuracies obtained using the bootstrapping method was higher than that of leave-one-out method. As in the 10-way classification model, the low level fungal-infected samples were mostly misclassified as another low level infected sample, and high level infected sample as another high level infected sample.

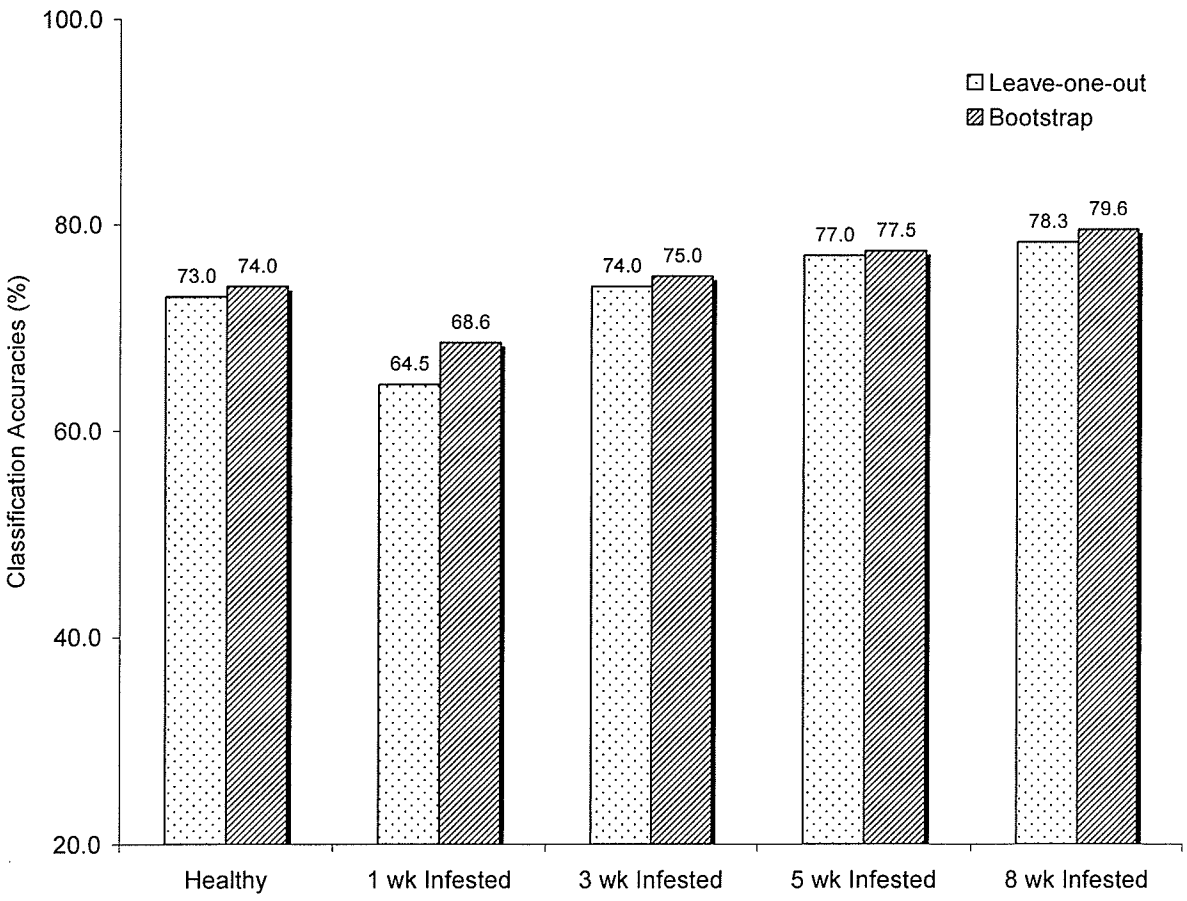

Figure 4.5 Classification accuracies of pair-wise LDA classification model for healthy and fungal-infected wheat samples based on their infestation levels using leave-one-out and bootstrapping validation techniques.

In another LDA analysis, the composite low level and composite high level fungal infected wheat samples were created by mixing all low infection samples (1 wk and 3 wk infection samples) together, and all high level infected samples (5 wk and 8 wk infection)together, respectively. These low and high level infected samples were analysed with the healthy samples by a 3-way LDA classifier, and the classification accuracies obtained using the leave-one-out and bootstrapping validation techniques for this analysis are given in Figure 4.5. Classification accuracies for healthy, low infected and highly infected samples were 78.0, 90.5, and 94.8%, respectively using leave-one-out method, and 79.8, 90.8, and 95.4% using the bootstrapping validation method. The misclassification between healthy and low level infected samples was relatively high (22.0%), and misclassification between low and highly infected grains was relatively low (5.0 – 5.8%).

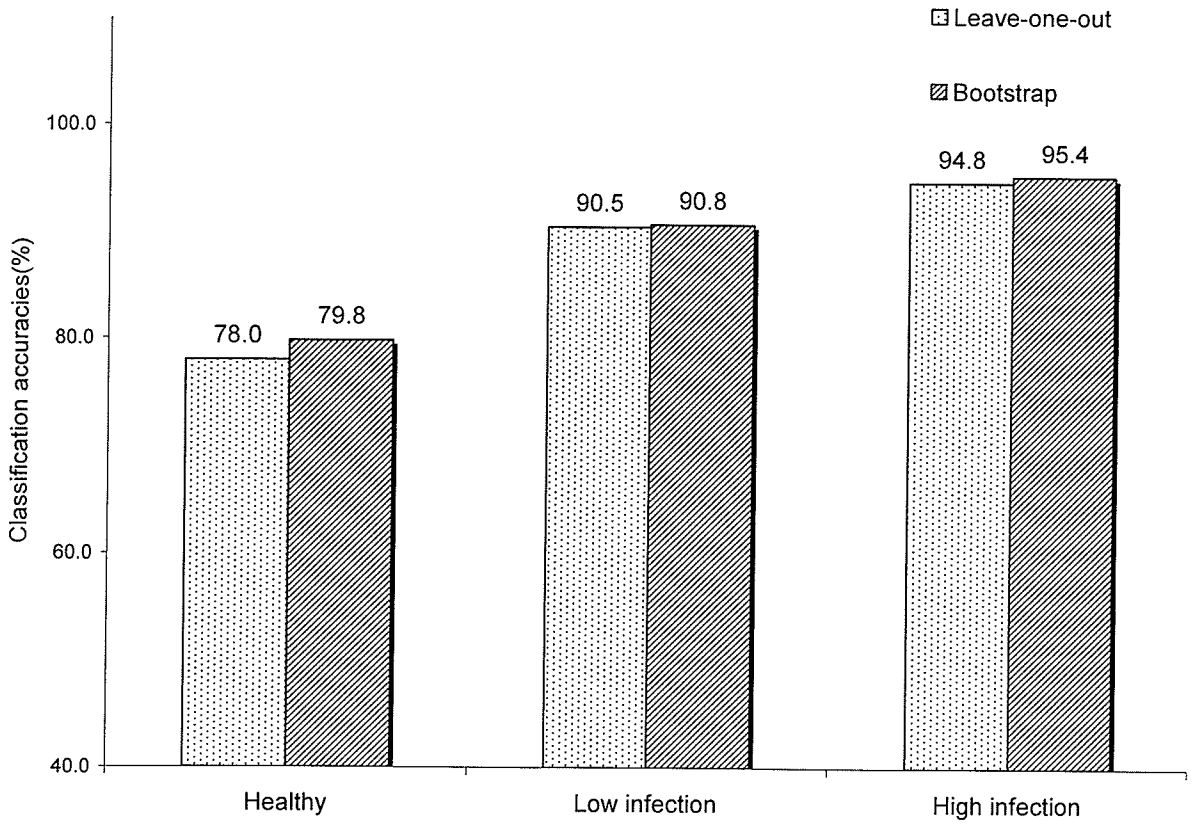

Figure 4.6 Classification accuracies of healthy, low and highly infected wheat samples using 3-way LDA classifier

4.5.5 Ranking of temperature features

Temperature features ranking was performed using the PROC STEPDISC in SAS (version 9.1.3, SAS Institute Inc., Cary, N.C). These features were ranked based on their contribution to the classification model, and ranking of these features with partial R^2 values are given in Table 4.5. STPEDISC procedure determines the ranking of various features based on the correlation coefficients and squared canonical correlation values (Majumdar and Jayas 2000a). There were many overlaps in ΔT_{Hstd}, and ΔT_{Cstd} in t statistics, but they ranked second and third after ΔT_{Hmean}. As shown in Table 4.5, there was more variation among the samples obtained by ΔT_{Hmean} and it came first in derived heating features, and ΔT_{Cstd} came first in derived cooling features.

Table 4.5 Ranking of derived temperature features of healthy and fungal infected wheat samples on the basis of their contribution to the LDA classifier using STEPDISC analysis.

No.	Derived temperature features	Partial R^2
1	ΔT_{Hmean}	0.64
2	ΔT_{Hstd}	0.36
3	ΔT_{Cstd}	0.20
4	ΔT_{Hmax}	0.19
5	$\Delta T_{Hmedian}$	0.14
6	ΔT_{Cmean}	0.14
7	ΔT_{Cmax}	0.08
8	$\Delta T_{Cmedian}$	0.05
9	ΔT_{Cmin}	0.05
10	ΔT_{Hmin}	0.05
11	ΔT_{Hmode}	0.03
12	ΔT_{Cmode}	0.01

4.6 Classification using QDA

PROC DISCRIM function in SAS (version 9.1.3, SAS Institute Inc., Cary, N.C) used to develop quadratic discriminant analysis (QDA) models for the classification of fungal infection in wheat samples. In total four different analyse were carried out by the QDA classifier: (i) 10-way classification, (ii) 3-way classification, (iii) pair-wise comparison, and (iv) classification based on infection level. For developing the QDA model, a total of 12 derived temperature features (6 from temperature rise data and 6 from temperature drop data) were used, and the leave-one-out method and bootstrapping validation techniques were used to validate the developed QDA model.

4.6.1 10-way classification

All the 10 samples were mixed together and the QDA classification model was developed from the derived temperature features. The classification accuracies of the developed QDA model using leave-one-out and bootstrapping methods are given in Figure 4.6. Healthy samples had the highest classification accuracies of 73.0 and 78.0% using the leave-one-out and bootstrapping methods, respectively. Among the fungal-infected samples, 8 wk *Penicillium* spp.-infected samples had higher classification accuracy using both validation techniques (60.0% using leave-one-out, and 71.1% using bootstrapping method). There were more misclassifications occurred between the different fungal species, and healthy samples were misclassified with low level fungal-infected samples. For all samples, classification accuracy of the QDA classifier using bootstrapping method was higher than that of leave-one-out method.

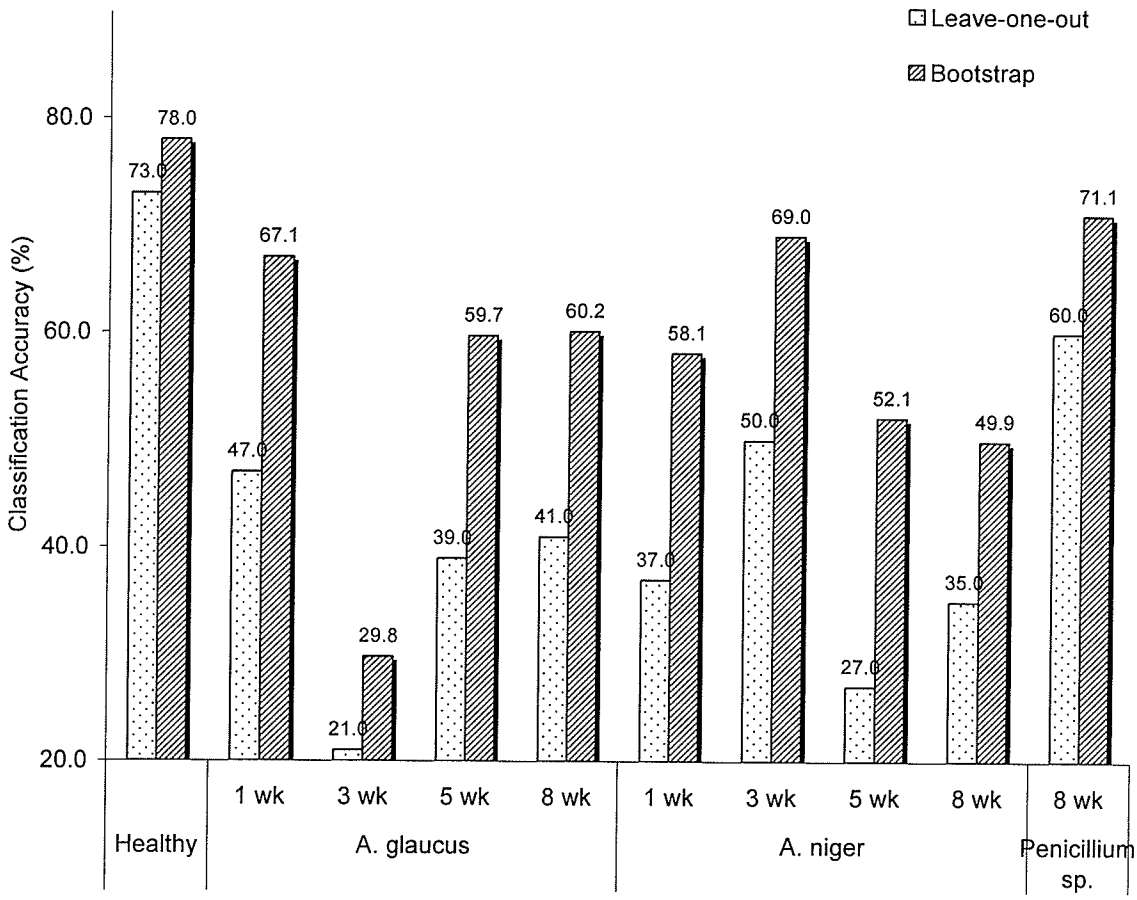

Figure 4.7 Classification accuracies of 10-way QDA classification model for healthy and fungal-infected wheat samples based on infestation level using leave-one-out and bootstrapping validation techniques.

4.6.2 3-way classification

In 3-way classification model, temperature features of healthy samples were compared with fungal-infected samples at the same infection level. Classification accuracies of 3-way classification QDA model using the leave-one-out and bootstrapping method is given in Figure 4.7. Classification accuracy of healthy grains was improved from 74.0 to 99.0%, from 1 wk of infection to 8 wk of infection using the leave-one-out method. Classification accuracy of *A. glaucus*-infected samples were in the range of 33.0 to 63.0%, and for *A. niger*-infected samples the classification accuracies were in the range of 48.0 to 66.0%, using the leave-one-out method. Using the bootstrapping method, the classification accuracies were in the range 45.0 to 85.1% and 60.9 to 83.0% for *A. glaucus*, and *A. niger*-infected samples, respectively. For *Penicillium* samples, classification accuracies of the QDA classifier were 63 and 76.0% using leave-one-out and bootstrapping methods, respectively. Bootstrapping method had higher classification accuracy than that of leave-one-out method in QDA classifier. These results also followed the same trend as the LDA model; there were more misclassification between the fungal species, and few misclassifications between the healthy and fungal-infected samples. Singh et al, (2007) observed relatively more misclassifications (20.0%) between *A. glaucus* and *Penicillium*-infected wheat kernels while using a QDA model developed from the near-infrared hyperspectral imaging data.

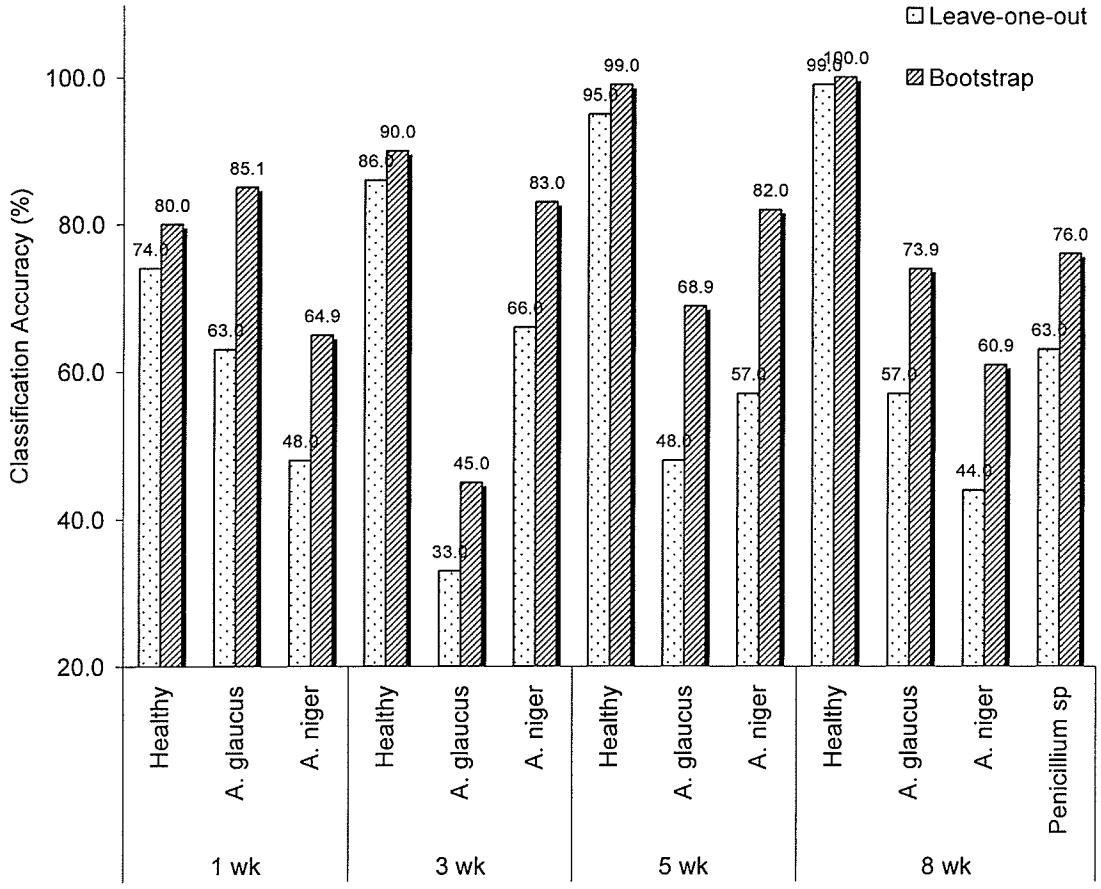

Figure 4.8 Classification accuracies of 3-way QDA classification model for healthy and fungal-infected wheat samples based on infection level using leave-one-out and bootstrapping validation techniques.

4.6.3 Pair-wise comparison

In QDA classification, there were two types of pair-wise comparisons carried out: (i) comparison between healthy and infected samples at every infection level; and (ii) comparison between healthy and particular fungal species infection at every infection level.

For the healthy versus infected classification model, the derived temperature data from all fungal species at the same infected level were mixed together and compared with the healthy samples. The classification accuracies of healthy versus infected samples at 4 different infection levels using leave-one-out and bootstrapping method are given in Figure 4.8. Classification accuracy of the 1 wk infection sample was 95.5% using leave-one-out method and 98.5% using the bootstrapping method. The healthy sample had classification accuracies of 79.0 and 82.0% using leave-one-out and bootstrapping methods, respectively, with 1 wk fungal-infected samples. But the classification accuracies of healthy samples increased to >93.0% when analysed with the fungal-infected samples beyond 3 wk of infection using bootstrapping method.

More than 90.0% accuracy was obtained from the QDA classifier using both validation techniques for infected samples. Classification accuracy of the healthy sample was above 90.0% from 3 wk of infection using bootstrapping method, and using the leave-one-out method 86.0% of accuracy was obtained when the healthy samples compared with 3 wk infected samples. Fungi use fatty acids in wheat grain for their growth. Decrease of FAV due to this action may create some changes in the temperature pattern of the grain during heating and cooling. These changes may be low at early stages

of infection and high at the fully infected stage. Because of these temperature pattern changes, the highly infected samples had more than 98.0% classification accuracy.

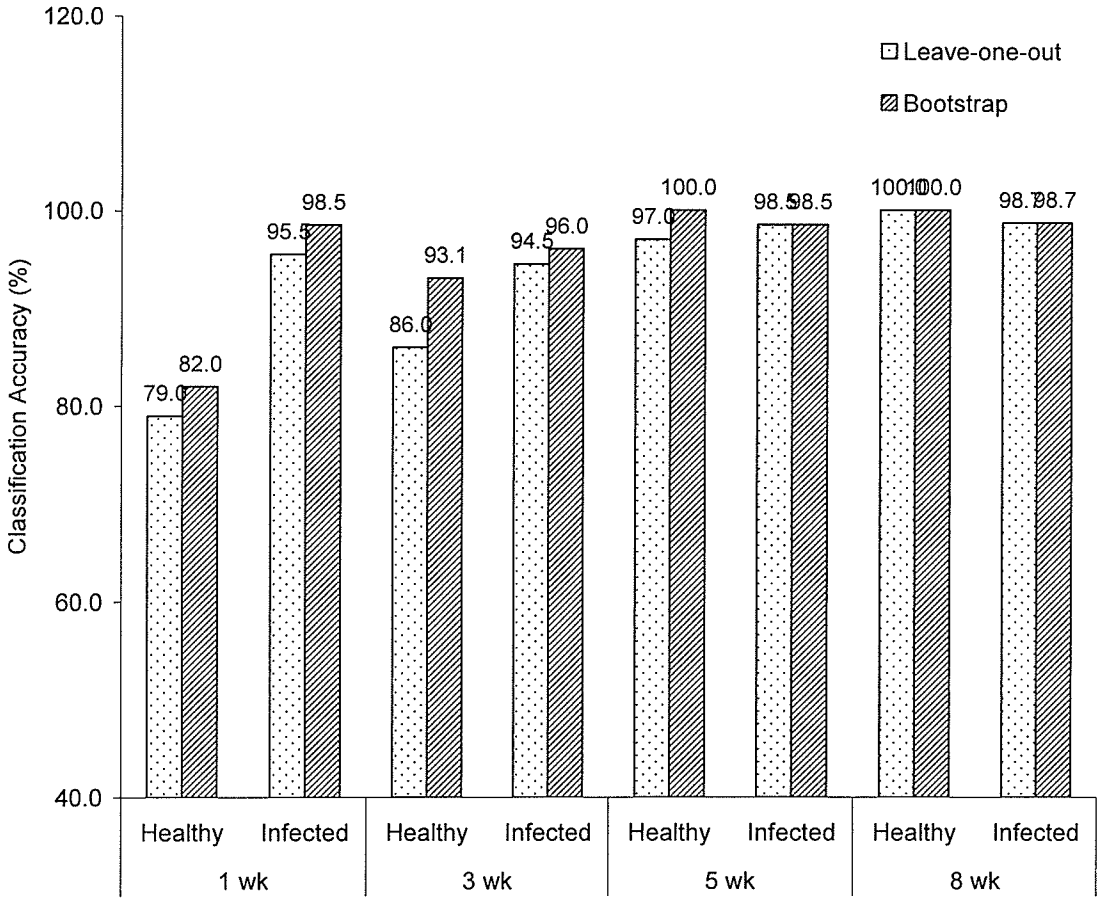

Figure 4.9 Classification accuracies of pair-wise QDA classification model for healthy and fungal-infected wheat samples based on infection level using leave-one-out and bootstrapping validation techniques.

In another pair-wise quadratic discriminant analysis function, wheat samples infected by the individual fungal species were compared with healthy grains. Leave-one-out and bootstrapping validation techniques were used for each analysis of *A. glaucus* infected versus healthy, *A. niger*-infected versus healthy and *Penicillium*-infected versus healthy wheat samples (Table 4.6 and 4.7). Classification accuracies varied from 83.0 to 100.0% for healthy grains using both validation methods. The samples infected with *A. glaucus* and *A. niger* were correctly classified more than 90.0 and 92.0% using both validation techniques from 1 wk of infection samples. Using the bootstrapping method, only 4.0 and 5.0% of misclassifications occurred between healthy and 3 wk *A. glaucus*-infected grains, and between healthy and 3 wk *A. niger*-infected the misclassification rates were 5.0 and 2.0%. Classification accuracies of the QDA classifier for the healthy and beyond 5 wk infected *Aspergillus* fungal species samples were 95.0% using both validation techniques. The 8 wk *Pencillium* spp.-infected samples had 99.0 and 100.0% classification accuracies, and all the healthy grains were correctly classified. Similar kinds of results were obtained by Singh et al. (2007) when identifying fungal infection in wheat kernels using near-infrared hyperspectral imaging system.

Table 4.6 Pair-wise discrimination of fungal infected wheat grains from healthy by quadratic discriminant analysis (QDA) using leave-one-out validation technique

	Classification accuracies at various infection periods (%)							
Fungi	1 wk		3 wk		5 wk		8 wk	
	A.glaucus	Healthy	*A.glaucus*	Healthy	*A.glaucus*	Healthy	*A.glaucus*	Healthy
A.glaucus	93.0	83.0	90.0	87.0	99.0	100.0	99.0	100.0
	A. niger	Healthy	*A. niger*	Healthy	*A. niger*	Healthy	*A. niger*	Healthy
A. niger	92.0	83.0	93.0	89.0	98.0	95.0	96.0	99.0
	Penicillium	Healthy	*Penicillium*	Healthy	*Penicillium*	Healthy	*Penicillium*	Healthy
Penicillium	-	-	-	-	-	-	99.0	100.0

Table 4.7 Pair-wise discrimination of fungal infected wheat grains from healthy by quadratic discriminant analysis (QDA) using bootstrapping validation technique

	Classification accuracies at various infection periods (%)							
Fungi	1 wk		3 wk		5 wk		8 wk	
	A.glaucus	Healthy	*A.glaucus*	Healthy	*A.glaucus*	Healthy	*A.glaucus*	Healthy
A.glaucus	98.0	90.0	95.0	96.0	99.0	100.0	100.0	100.0
	A. niger	Healthy	*A. niger*	Healthy	*A. niger*	Healthy	*A. niger*	Healthy
A. niger	96.0	83.0	98.0	95.0	99.0	98.0	99.0	100.0
	Penicillium	Healthy	*Penicillium*	Healthy	*Penicillium*	Healthy	*Penicillium*	Healthy
Penicillium	-	-	-	-	-	-	100.0	100.0

4.6.4 Comparison based on infection level

All fungal infected samples at same infection periods were mixed and compared with healthy samples using a 5-way QDA classifier. Validation of the developed QDA model was done using 2 different techniques, namely: leave-one-out and bootstrapping methods. Classification accuracies of the QDA classifier using both validation techniques are shown in Figure 4.9. The highest accuracy of 78.0% was obtained for healthy and fungal infected samples using leave-one-out method and using bootstrapping method, the highest accuracies were 82.0% and 80.3% for healthy and infected grains, respectively. All the misclassifications of healthy into infected samples were occurred between healthy and 1 wk infected samples (18.0%). Only about 4.0% of 1 wk infected grains were misclassified with all other samples except 3 wk infected sample, and only 6.6% of 8 wk infected samples were misclassified with all other samples except 5 wk infected sample.

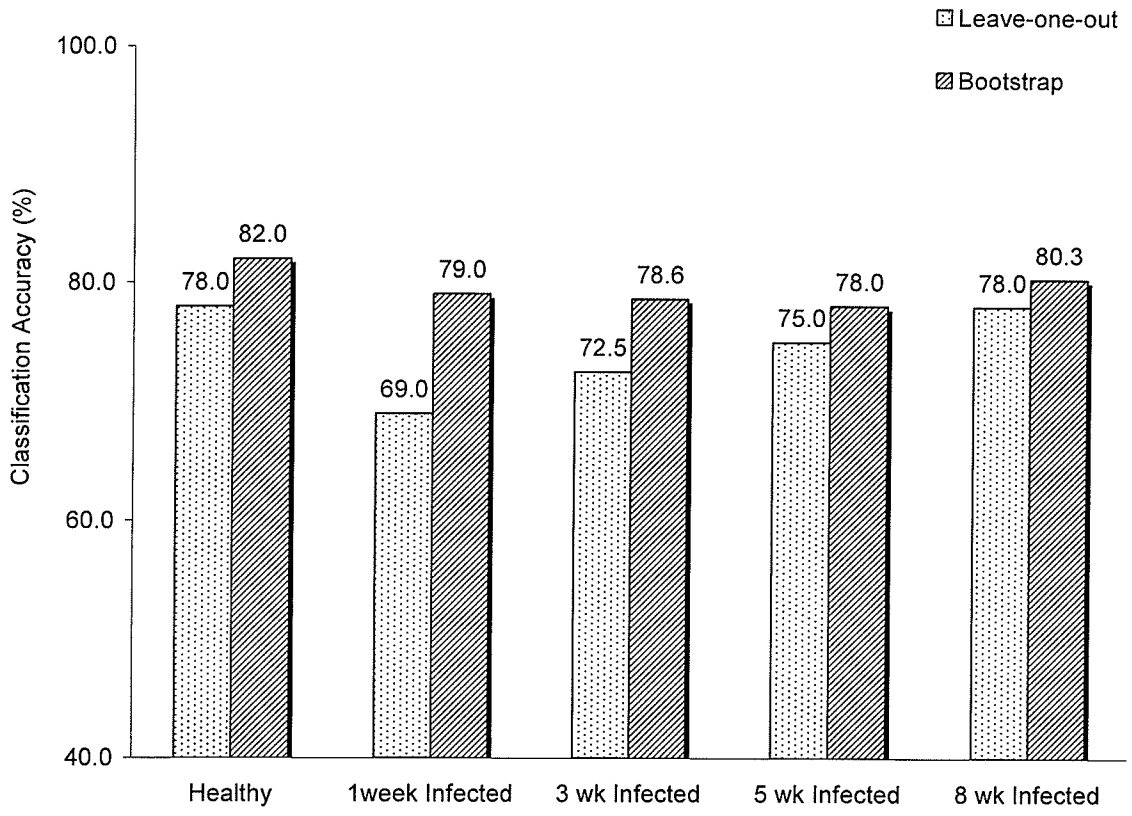

Figure 4.10 Classification accuracies of QDA classification model for healthy and fungal-infected wheat samples based on infection levels using leave-one-out and bootstrapping validation techniques.

In another QDA analysis, the composite low level infected wheat samples were created by mixing all low infection samples (1 wk and 3 wk infection samples), and another composite high infection sample was made by mixing all high level infected samples (5 and 8 wk infection)together. These composite low and high level samples were analysed with the healthy samples, and the classification accuracies obtained by the 3-way QDA classifier using leave-one-out and bootstrapping validation techniques for this analysis is given in Figure 4.10. Classification accuracies for healthy, low infected and highly infected samples were 85.0, 90.5, and 93.8%, respectively using both validation methods. Here also, healthy samples were misclassified as low infected samples (about 21.0%), but the misclassification between healthy and highly infected grains was relatively low (1.2%), and only 5.4% of the low infected samples were misclassified as high infected grains.

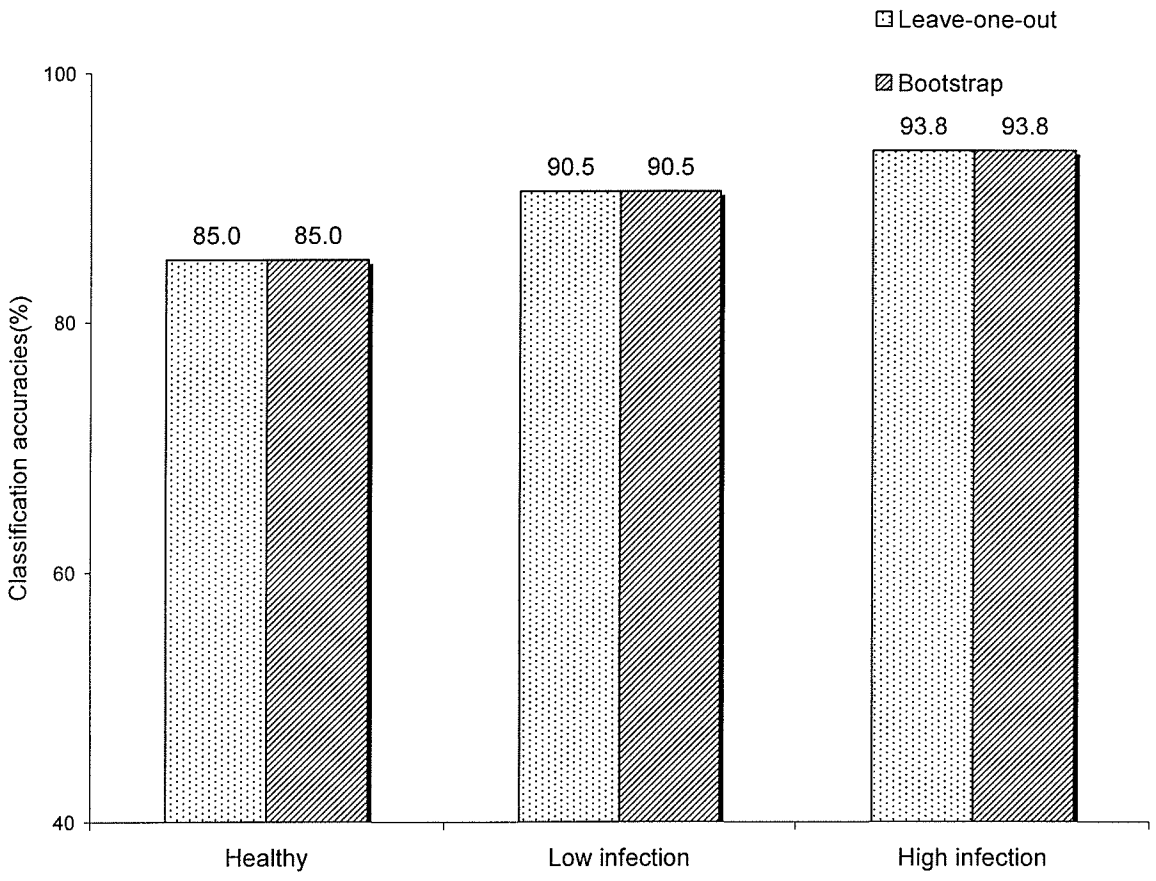

Figure 4.11 Classification accuracies of 3-way QDA classifier based on fungal infection levels.

4.6.5 Ranking of temperature features

The derived temperature features were ranked based on their contribution to the quadratic discriminant classification model using PROC STEPDISC function in SAS, and the ranking and partial R^2 values of these features are given in Table 4.8. In QDA model, ΔT_{Hmean} ranked first with a partial R^2 of 0.64, and ΔT_{Cmode} got 2nd rank. Out of 6 top most features, 3 were from derived heating data and another 3 from derived cooling data, and ΔT_{Cmode} came first in derived cooling features.

Table 4.8 Ranking of derived temperature features of healthy and fungal infected wheat samples on the basis of their contribution to the QDA classifier using STEPDISC analysis.

No.	Derived temperature features	Partial R^2
1	ΔT_{Hmean}	0.64
2	ΔT_{Cmode}	0.36
3	ΔT_{Cstd}	0.20
4	ΔT_{Hmin}	0.19
5	ΔT_{Cmean}	0.14
6	ΔT_{Hmax}	0.14
7	$\Delta T_{Hmedian}$	0.08
8	ΔT_{Cmax}	0.05
9	ΔT_{Hstd}	0.05
10	ΔT_{Hmode}	0.05
11	ΔT_{Cmin}	0.03
12	$\Delta T_{Cmedian}$	0.01

Chapter 5

CONCLUSION

The results from this study indicate that thermal imaging could be a promising machine vision technique to detect fungal infection in stored wheat grain. The rate of heating and cooling of the fungal-infected grains was slightly higher than that of healthy kernels. In total, 12 derived temperature features were used for classifying healthy and fungal-infected wheat samples. Linear and quadratic discriminant analysis with two different validation techniques, i.e., leave-one-out and bootstrapping methods were used for classification. Classification accuracies of 90.0-100.0% and 95.5-99.0% were obtained for healthy and fungal-infected samples, respectively, using the pair-wise LDA classifier 3 wk or longer infection. In the QDA classifier, classification accuracies were 86.0-100.0% and 94.5-98.7% for healthy and infected samples, respectively. In the pair-wise comparison between healthy and each fungal species infected samples, the LDA classifier yielded an accuracy of >91.0% for healthy, >95.0% for *A. glaucus*-infected, and >94.0% for *A. niger*-infected samples beyond 3 wk of infection. The pair-wise classification results indicated that the linear discriminant classifier gave comparatively better results than the quadratic discriminant classifier.

When classifying *A. glaucus*, *A. niger* and *Penicillum*-infected grains at different infection periods both classifiers gave relatively low accuracies (25.0 to 71.9%) using leave-one-out and bootstrapping validation methods. Most of the misclassifications happened between the fungal species at the same level of infection. Three way LDA and QDA classifiers yielded >90% classification accuracies using leave-one-out and bootstrapping validation methods for low and highly infected grains, and relatively low results (78.0 – 85.0%) for healthy grains.

The early detection (3 wk) of fungal infection leads to initiation of control measures to prevent the grain deterioration and quality loss. The results prove that thermal imaging system could be a useful tool to find out whether the grain is infected by fungi or not and the level of infection (low or high). But, fungal species differentiation was not possible because the temperature profiles of the wheat samples infected by different fungal species were similar probably due to the insignificant changes in the chemical components.

The feasibility of using the thermal imaging system to detect field fungi such as *Fusarium* spp.-infected grains will be studied in the future. With this work, we were able to develop an overall idea about fungal infection in wheat. It could also be possible to use thermal imaging technique to detect fungal infection in different cereal crops other than wheat. In the future, combinations of insect and fungal infestation levels in cereal grains can be studied using thermal imaging.

REFERENCES

Abram, S.E., C.B. Asiddao and A.C. Reynolds. 1980. Increased skin temperature during transcutaneous electrical stimulation. *Anesthesia and Analgesia* 59(1): 22–25.

Abramson, D., R.N. Sinha and J.T. Mills. 1980. Mycotoxin and odour formation in moist cereals during granary storage. *Cereal Chemistry* 57: 346-351.

Agerskans, J. 1975. Thermal imaging – A technical review. In Proceedings of Temperature Measurement, 375 – 388. London. April 9 -11.

Amalric, R., H. Brondone, F. Robert, C. Altschuler, J.M. Spitalier, J. Ingrand and J. Deschanel. 1978. Dynamic telethermography of 2,200 breast cancers. *Acta Thermographica* 3: 46-52.

Anderson, J.D. 1970. Physiological and biochemical differences in deteriorating barley seed. *Crop Science* 10: 36-39.

Anonymous. 2007. About thermal Imaging. http://www.temperatures.com/thermal imaging.html (2007/12/ 10).

Arenas, A.J., F. Gomez, R. Salas, P. Carrasco, C. Borge, A. Maldonado, D.J. O'Brien and F.J.M. Moreno. 2002. An Evaluation of the application of infrared thermal

imaging to the tele-diagnosis of sarcoptic mange in the Spanish ibex (*Capra pyrenaica*). *Veterinary Parasitology* 109: 111-117.

Berliner, P., D.M. Oosterhuis and G.C. Green. 1984. Evaluation of the infrared thermometer as a crop stress detector. *Agricultural and Forest Meteorology* 31 (3-4): 219-230.

Bourjat, P., M. Gautherie and E. Grosshans. 1975. Diagnosis, follow-up and prognosis of malignant melanomas by thermography. *Bibliotheca Radiologica* 6: 115-127.

Brelsford, K.L. and S. Uematsu. 1985. Thermographic presentation of cutaneous sensory and vasomotor activity in the injured peripheral nerve. *Journal of Neurosurgery* 62(5): 711-715.

Brooks, J.P., W.B. Perry, A.T. Putnam and R.E. Karulf. 2000. Thermal imaging in the detection of bowel ischemia. *Diseases of the Colon and Rectum* 43(9): 1319-1321.

Chaerle, L., W. van Caeneghem, E. Messens, H. Lambers, M. van Montagu, and D. van der Straeten. 1999. Presymptomatic visualisation of plant–virus interactions by thermography. *Nature Biotechnology* 17: 813–816.

Chang, T.C., Y.L. Hsiao and S.L. Liao. 2008. Application of digital infrared thermal imaging in determining inflammatory state and follow-up effect of methypredisolone pulse therapy in patients with Graves' ophthamopathy. *Graefe's Archive for Clinical and Experimental Ophthalmology* 246(1): 45-49.

Christensen, C.M., and H.H. Kaufmann. 1969. Grain Storage: The role of fungi in quality loss 1st edition. 17-35. Minneapolis, MN: University of Minnesota Press.

Collins, A.J., E.F.J. Ring, J.A. Cosh and P.A. Bacon. 1974. Quantitation of thermography in arthritis using multi-isothermal analysis. I. The thermographic index. *Annals of Rheumatic Dieeases* 33(2): 113-115.

Cristofolini, M., F. Piscioli, C. Valdinotti and A.D. Selva. 1976. Correlations between thermography and morphology of primary cutaneous malignant melanomas. *Acta Thermographica* 1: 3-11.

Danno, A., M. Miyazato and E. Ishiguro. 1978. Quality evaluation of agricultural products by infrared imaging method: Grading of fruits for bruise and other surface detects. *Memoris of the Faculty of Agriculture*, Kagoshima University 14: 123-138.

Danno, A., M. Miyazato and E. Ishiguro. 1980. Quality evaluation of agricultural products by infrared imaging method: Maturity evaluation of fruits and vegetables. *Memoris of the Faculty of Agriculture*, Kagoshima University 16: 157-164.

Dauncey, M. J., and D.L. Ingram. 1983. Evaluation of the effects of environmental temperature and nutrition on growth and development. *Journal of Agricultural Sciences* 101: 351-358.

Davis, A.P. and A.H. Lettington. 1988. Principles of thermal imaging. In *Applications of Thermal Imaging*, eds. S.G. Burnay, T.L. Williams and C.H. Jones, 1-34. Bristol, UK: IOP Publications Limited.

Delwiche, S. R. 2003. Classification of scab- and other mold-damaged wheat kernels by near-infrared reflectance spectroscopy. *Transactions of the ASAE* 46(3): 731-738.

Donald, W.W. and C.J. Mirocha. 1977. Chitin as a measure of fungal growth in stored corn and soybean seed. *Cereal Chemistry* 54(2): 466-474.

Dowell, E.E., T.C. Pearson, E.B. Maghirang, F. Xie, and D.T. Wicklow. 2002. Reflectance and transmittance spectroscopy applied detecting fumonisin in single corn kernels infected with *Fusarium verticillioides. Cereal Chemistry* 79(2): 222-226.

Egnell, G. and G. Orlander. 1993. Using infrared thermography to assess viability of pinus sylvestris and picea abies seedlings before planting. *Canadian Journal of Forest Research* 23(9): 1737-1743.

FAOSTAT. 2007. Food and Agriculture Organizations of United Nations. http://www.faostat.fao.org (2007/10/24).

Farag, R.S., F.A. Khallil, S.M. Mohsen and A.E. Bosyony. 1985. Effect of certain fungi on the lipids contents of wheat kernels, sesame and soybean seeds. *Grasas Aceites* 36: 362-367.

FAS. 2007. United States Department of Agriculture. http://www.fas.usda.gov (2007/12/05).

Fitzgerald, G.J., D. Rodriguez, L.K. Christensen, R. Belford, V.O. Sadras and T.R. Clarke. 2006. Spectral and thermal sensing for nitrogen and water status in rainfed and irrigated wheat environments. *Precision Agriculture* 7: 233-248.

Fuchs, J. 2002. Thermography used in diagnosis of horses' locomotor injuries. http://www.infraredtraining.com. (2007/10/04)

Gaussorgues, G. 1994. Infrared Thermography. In *Microwave Technology*: Series 5. London: Kluwer Academic Publishers.

Gonzalez, R.C. and R.E. Woods. 2002. In *Digital Image Processing*, 2nd edition. 44-45. Delhi, India: Pearson Education Private Limited.

Gros, C. and M. Gautherie. 1980. Breast thermography and cancer risk prediction. *Cancer* 45(1): 51-56.

Hellebrand, H.J., H. Beuche and M. Linke. 2002. Thermal imaging: A promising high-tech method in agriculture and horticulture. In *Physical Methods in Agriculture* : *Approach to Precision and Quality*, eds. J. Blahovec and M. Kutilek, 411-427. New York, NY: Kluwer Academic/ Plenum Publishers.

Hellebrand, H.J., U. Brehme, H. Beuche, U. Strollbergh and H. Jacobs. 2003. Application of thermal imaging for cattle management. In Programme book of the *Fourth European Conference on Precision Agriculture and Precision Livestock Farming*. Berlin, Germany. July 15-19, eds. A. Werner and A. Jarfe. 312-316. Wageningen, The Netherlands: Wageningen Academic Publishers.

Hellebrand, H.J., W.B. Herppich, H. Beuche, K.H. Dammer, M. Linke, and K. Flath. 2006. Investigations of plant infections by thermal vision and NIR imaging. *International Agrophysics* 20: 1-10.

Inoue, Y. 1990. Remote detection of physiological depression in crop plants with infrared thermal imagery. *Japanese Journal of Crop Science* 59(4): 762-768.

Ivanitsky, G.R., E.P. Khizhnyak, A.A. Deev, and L.N. Khizhnyak. 2005. Thermal imaging in medicine: A comparative study of infrared systems operating in

wavelength ranges of 3–5 and 8–12 μm as applied to diagnosis. *Doklady Biochemistry and Biophysics* 407(1): 59-63.

Jain. P.C., J. Lacey, and L.Stevens. 1991. Use of API-Zym strips and 4-nitrophenyl susstrates to detect and quantify hydrolytic enzymes in media and grain colonised by *Aspergillus*, *Euritium* and *Penicillium* spp. *Mycological Research* 95:834-842.

Jarvis, B., D.A.L. Seiller, A.J.L. Ould and A.P. Williams. 1984. Observations on the enumeration of molds in food and feeding stuffs. *Journal of Applied Bacteriology* 55: 325-336.

Jones, C.H., W.B. Greening, J.B. Davey, J.A. McKinna and V.J. Greeves. 1975. Thermography of the female breast: a five-year study in relation to the detection and prognosis of cancer. *The British Journal of Radiology* 48(571): 532-538.

Jones, C.H., E.F.J. Ring and R.P. Clark. 1988. Medical thermography. In *Applications of Thermal imaging*, ed. S.G. Burnay, T.L. Williams and C.H.Jones.156-187. Bristol, UK: IOP Publications Ltd.

Jones, H.G. 1999. Use of infrared thermometry for estimation of stomatal conductance as a possible aid to irrigation scheduling. *Agricultural and Forest Meteorology* 95: 139-149.

Jones, H.G., M. Stoll, T. Santos, C.D. Sousa, M.M. Chaves and O.M. Grant. 2002. Use of infrared thermography for monitoring stomatal closure in the field: application to grapevine. *Journal of Experimental Botany* 53(378): 2249-2260.

Jones, S.M. and R.A. Avery. 1989. The use of a pyroelectric vidicon infrared-red camera to monitor the body temperature of small terrestrial vertebrates. *Functional Ecology* 3(3): 373-377.

Kalma, J.D. and D.L.B. Jupp .1990. Estimating evaporation from pasture using infrared thermometry: evaluation of a one-layer resistance model. *Agricultural and Forest Meteorology* 51: 223 – 246

Kastberger, G. and R. Stachil. 2003. Infrared imaging technology and biological applications. *Behavior Research Methods, Instruments and Computers* 35 (3): 429-439.

Keshri, G., N. Magan and P. Voysey, 1998. Use of an electronic nose for the early detection and differentiation of spoilage fungi. *Letters in applied microbiology* 27: 261-264.

Keshri, G. and N. Magan. 2000. Detection and differentiation between mycotoxigenic and non-mycotoxigenic strains of two *Fusarium* spp. using volatile production profiles and hydrolytic enzymes. *Journal of Applied Microbiology* 89: 825-833

Kim, Y.H. and S.H. Lee.2004. Thermal and visual image characteristics of potato transplants as affected by photosynthetic photon flux and electric conductivity. ASAE Paper no: 044101. St. Jospeh, MI: ASAE.

Lacey, J., S.T. Hill and M.A. Edwards. 1980. Micro organisms in stored grains : their enumeration and significance. *Tropical Stored Product Information* 39: 19-33.

Lacey, J., A. Hamer and N. Magan. 1994. Respiration and losses in stored wheat under different environmental conditions. In *Stored Product Protection* eds. Highley, E.,

E.J. Wright, H.J. Banks, and B.R. Champ. 1007-1013. Wallingford: CAB International.

Lamprecht, I., E. Schmolz, L. Blanco and C.M. Romero. 2002a. Energy metabolism of the thermogenic tropical water lily, *Victoria cruziana. Thermochimica Acta* 394: 191-204.

Lamprecht, I., E. Schmolz, L. Blanco, and C.M. Romero. 2002b. Flower ovens: thermal investigations on heat producing plants. *Thermochimica Acta.*391: 107-118.

Lancaster, W.C., S.C. Thomson and J.R. Speakman. 1997. Wing temperature in flying bats measured by infrared thermography. *Journal of Thermal Biology* 22 (2): 109-116.

Lin H.H. and M.A. Cousin. 1985. Detection of mould in processed food by high performance liquid chromatography. *Journal of Food Protection* 48: 671-678.

Madhyastha, S., R.R. Marquardt and D. Abramson. 1993. Effect of *ochratoxin*-producing fungi on the chemical composition of wheat and barley. *Journal of Food Quality* 16(4): 287-299.

Majumdar, S. and D.S.Jayas. 2000. Classification of cereal grains using machine vision: I. Morphology models. *Transactions of ASAE* 43(6): 1669-1675.

Magan, N. 1993. Early detection of fungi in stored grain. *International Biodeterioration and Biodegradation* 32: 145-160.

Manickavasagan, A. 2007. Thermal imaging for potential use in cereals and oilseeds handling. Unpublished Ph.D. thesis. Winnipeg, MB: Department of Biosystems Engineering. Universoty of Manitoba.

Meinlschmidt, P. and V. Margner. 2003. Thermographic techniques and adopted algorithms for automatic detection of foreign bodies in food. In *Proceedings of Thermosense XXV*, 168-177. Bellingham, WA: The International Society for Optical Enginnering.

Muir, W.E. and N.D.G. White. 2001. Microorganisms in stored grain. In *Grain Preservation Biosytems* ed. W.E. Muir, 28 - 42. Winnipeg, MB: Department of Biosystems Engineering, University of Manitoba.

Nilsson, H.E. 1995. Remote sensing and image analysis in plant pathology. *Canadian Journal of Plant Pathology* 17: 154-166.

Pearson, T.C., D.T. Wicklow, E.B. Maghirang, F. Xie and F.E. Dowell. 2001. Detecting *aflatoxin* in single corn kernels by using transmittance and reflectance spectroscopy. *Transactions of the ASAE* 44(5): 1247-1254.

Pearson, T.C., D.T. Wicklow and M.C. Pasikatan. 2004. Reduction of a*flatoxin* and fumonosine contamination in yellow corn by high speed duel wave-length sorting. *Cereal Chemistry* 81(4): 490-498.

Pearson, T.C., and D.T. Wicklow. 2006. Detection of corn kernels infected by fungi. *Transactions of the ASAE* 49(4): 1235-1245.

Pomeranz, Y. 1992. Biochemical, functional, and nutritive changes during storage. In *Storage of Cereal Grains and Their Products,* 4th edition ed. D.B. Sauer, 55-118. St. Paul, MN: American Association of Cereal Chemists.

Ride J.P. and R.B. Drysdale. 1972. A rapid method for the chemical estimation of filamentous fungi in plant tissue. *Physiology and Plant Pathology* 2: 7-15.

Schnurer, J., J. Olsson and T. Borjesson.1999. Fungal volatiles as indicators of food and feeds spoilage. *Fungal Genetics and Biology* 27: 209–217.

Scotter, J.M., V.S. Langford, P.F. Wilson, M.J. McEwan and S.T. Chambers. 2005. Real-time detection of common microbial volatile organic compounds from medically important fungi by Selected Ion Flow Tube-Mass Spectrometry (SIFT-MS). *Journal of Microbiological Methods* 63(2): 127-134.

Singh, C.B., D.S. Jayas, J. Paliwal and N.D.G. White. 2007. Fungal detection in wheat using near-infrared hyprespectral imaging. *Transactions of the ASAE* 50(6): 2171-2176.

Singh, R.P. and D.R. Heldman. 1993. *Introduction to Food Engineering*, 2nd edition. San Diego, CA. Academic Press Inc.

Smith, E.A., E. Chambers and S. Colley. 1994. Development of vocabulary and references for describing off-odors in raw grains. *Cereal Foods World* 39: 495-499.

Stajnko, D., M. Lakota and M. Hocevar. 2004. Estimation of number and diameter of apple fruits in an orchard during the growing season by thermal imaging. *Computers and Electronics in Agriculture* 42: 31-42.

Stoll, B.A. 1974. Endocrine adjuvant therapy in breast cancer. *Bibliotheca Radiologica* 6: 178-184.

Tan, T.Z., C. Quek, G.S. Ng and E.Y.K. Ng. 2007. A novel cognitive interpretation of breast cancer thermography with complementary learning fuzzy neural memory structure. *Expert Systems with Applications* 33: 652-666.

Tipples, K.H., 1995. Quality and nutritional changes in stored grain. In *Stored-grain Ecosystems* eds. D.S. Jayas, N.D.G. White and W.E. Muir. 189–202. New York , NY: Marcel Dekker, Inc.

Tothill, I.E., D. Harris, and N. Magan. 1992. The relationship between fungal growth and ergosterol in wheat grain. *Mycological Research* 11: 965-970.

Touloukian, Y.S and D.P. DeWitt. 1972. Thermal radiative properties – Non-metallic solids. In *Thermophysical Properties of Matter* 178-195. New York, NY. IFI / Plenum Publishers.

Tseng, T.C., J.C. Tu and S.S. Tzean. 1995. Mycroflora and mycotoxins in dry bean (*Phaseolus vulgaris*) produced in Taiwan and in Ontario, Canada. *Botanical Bulletin of Academia Sinica* 36: 229-234.

Turco, M.R.D., R. Santoni, S. Ciatto and E. Fallico. 1982. The role of infrared thermography, mammography and physical examination in the diagnosis of breast cancer. *Acta Thermographica* 7: 86-91.

Vadivambal, R., D.S. Jayas, V. Chelladurai and N.D.G. White. 2007. Temperature distribution studies in microwave heated grains. Paper no: RRV-07100. CSBE/ASABE North-Central Intersectional Conference. Fargo, ND.

Varith, J., G.M. Hyde, A.L. Baritelle, J.K. Fellman and T. Sattabongkot. 2003. Non-contact bruise detection in apples by thermal imaging. *Innovative Food Science and Emerging Technologies* 4: 211-218.

Veraverbeke, E.A., P. Verboven, J. Lammertyn, P. Cronje, J.D. Baerdemaeker, and B.M. Nicolai. 2003. Thermographic surface quality evaluation of apple. ASAE paper no: 036207.St.Jospeh, MI: ASAE.

Walcott, R.R., D.C. McGee and M.K. Mishra. 1998. Detection of asyptomatic fungal infections of soybean seeds by ultrasound analysis. *Plant Disease* 82(5): 584-589.

Wang, D., F.E. Dowell, M.S. Ram and W.T. Schapaugh. 2003. Classification of fungal-damaged soybean seeds using near-infrared spectroscopy. *International Journal of Food Preporties* 7: 75-82.

White, N.D.G. 1995. Insects, mites and insecticides in stored-grasin ecosystems. In Stored-Grain Ecosystems, eds. D.S. Jayas, N.D.G. White and W.E. Muir, 123-167. New York, NY: Marcel Decker Inc.

Williams, A.P. 1989. Methodology developments in food mycology. *Journal of Applied Bacteriology* 67(5): 612-617.

Wolfe, W.L. and G.J. Zissis. 1978. In *The Infrared Handbook.* 78-82. Washington, DC. Office of Naval Research.

Zsom, T., W.B. Herppich, C.S. Bala, A. Fekete, J. Felfoldi and M. Linke. 2005. Study of water transpiration features of sweet pepper using a thermal imaging system and non-destructive quality monitoring during post-harvest storage. *Journal of Thermal Analysis and Calorimetry 82*: 239-243.

APPENDIX

Confusion matrices

Table A.1 Confusion matrix (in %) for the 10-way LDA model using leave-one-out method

Sample (To) → / (From) ↓	AG 1wk	AG 3wk	AG 5wk	AG 8wk	AN 1wk	AN 3wk	AN 5wk	AN 8wk	Pen 8wk	Healthy
AG 1wk	30.0	15.0	1.0	0.0	36.0	14.0	1.0	0.0	1.0	2.0
AG 3wk	10.0	34.0	0.0	4.0	10.0	37.0	3.0	0.0	0.0	2.0
AG 5wk	0.0	0.0	61.0	8.0	1.0	0.0	20.0	1.0	8.0	1.0
AG 8wk	1.0	0.0	12.0	43.0	1.0	0.0	6.0	22.0	15.0	0.0
AN 1wk	23.0	8.0	0.0	4.0	49.0	7.0	1.0	3.0	2.0	3.0
AN 3wk	8.0	17.0	0.0	4.0	6.0	60.0	1.0	1.0	0.0	3.0
AN 5wk	1.0	1.0	18.0	12.0	2.0	1.0	45.0	11.0	9.0	0.0
AN 8wk	3.0	2.0	4.0	24.0	1.0	0.0	8.0	46.0	12.0	0.0
Pen 8wk	0.0	1.0	0.0	9.0	0.0	4.0	3.0	14.0	69.0	0.0
Healthy	5.0	0.0	0.0	0.0	24.0	0.0	0.0	0.0	0.0	71.0

Table A.2 Confusion matrix (in %) for the 10-way LDA model using bootstrapping method

Sample (To) → / (From) ↓	AG 1wk	AG 3wk	AG 5wk	AG 8wk	AN 1wk	AN 3wk	AN 5wk	AN 8wk	Pen 8wk	Healthy
AG 1wk	29.0	13.0	1.1	0..0	37.9	14.9	1.1	0.0	1.0	2.0
AG 3wk	11.0	33.1	0.0	4.0	8.9	38.1	3.0	0.0	0.0	1.9
AG 5wk	0.0	0.0	58.7	8.1	1.0	0.0	22.1	1.0	8.0	1.1
AG 8wk	1.0	0.0	11.8	44.0	1.0	0.0	6.0	22.1	14.0	0.0
AN 1wk	23.9	8.9	0.0	4.1	47.1	7.0	0.9	3.0	2.0	3.1
AN 3wk	8.0	18.0	0.0	3.9	5.9	59.0	1.1	1.1	0.0	3.0
AN 5wk	1.0	1.0	17.9	12.0	2.1	1.0	45.1	11.0	8.9	0.0
AN 8wk	3.0	2.0	4.1	23.0	1.0	0.0	7.9	46.9	12.1	0.0
Pen 8wk	0.0	1.0	0.0	9.0	0.0	3.9	3.0	14.0	69.1	0.0
Healthy	5.1	0.0	0.0	0.0	23.0	0.0	0.0	0.0	0.0	71.9

Table A.3 Confusion matrix (in %) for the 5-way LDA model using leave-one-out method

Sample (To) → / (From) ↓	1wk infected	3wk infected	5wk infected	8wk infected	Healthy
1wk infected	68.5	23.0	1.5	3.0	4.0
3wk infected	16.5	75.0	2.0	3.5	3.0
5wk infected	2.0	1.0	77.5	19.0	0.5
8wk infected	2.0	3.0	15.7	79.3	0.0
Healthy	26.0	0.0	0.0	0.0	74.0

Table A.4 Confusion matrix (in %) for the 5-way LDA model using bootstrapping method

Sample (To) → / (From) ↓	1wk infected	3wk infected	5wk infected	8wk infected	Healthy
1wk infected	68.6	22.9	1.5	3.0	4.0
3wk infected	17.1	75.0	1.9	3.5	2.5
5wk infected	2.0	1.0	77.5	19.0	0.5
8wk infected	2.0	3.0	15.4	79.6	0.0
Healthy	26.0	0.0	0.0	0.0	74.0

Table A.5 Confusion matrix (in %) for the 3-way LDA model using leave-one-out method

Sample (To) → / (From) ↓	1 wk			3 wk			5wk			8wk			
	A. glaucus	*A. niger*	Healthy	*A. glaucus*	*A. niger*	Healthy	*A. glaucus*	*A. niger*	Healthy	*A. glaucus*	*A. niger*	Healthy	*Penicillium*
A. glaucus	61.0	36.0	3.0	46.0	50.0	4.0	61.0	37.0	2.0	52.0	29.0	0.0	19.0
A. niger	47.0	46.0	7.0	43.0	53.0	4.0	36.0	62.0	2.0	33.0	50.0	2.0	15.0
Healthy	11.0	17.0	72.0	7.0	4.0	89.0	1.0	0.0	99.0	1.0	1.0	97.0	1.0
Penicillium	-	-	-	-	-	-	-	-	-	12.0	19.0	0.0	71.0

Table A.6 Confusion matrix (in %) for the 3-way LDA model using bootstrapping method

Sample (To) → / (From) ↓	1 wk			3 wk			5wk			8wk			
	A. glaucus	*A. niger*	Healthy	*A. glaucus*	*A. niger*	Healthy	*A. glaucus*	*A. niger*	Healthy	*A. glaucus*	*A. niger*	Healthy	*Penicillium*
A. glaucus	64.9	33.1	2.0	55.1	41.9	3.0	66.8	32.2	1.0	59.0	23.0	0.0	18.0
A. niger	38.9	57.0	4.1	37.0	59.0	4.0	32.9	65.1	2.0	31.0	52.1	0.0	14.9
Healthy	5.0	16.0	79.0	7.0	3.0	90.0	0.0	0.0	100.0	0.0	1.0	98.0	1.0
Penicillium	-	-	-	-	-	-	-	-	-	11.0	15.0	0.0	74.0

Table A.7 Confusion matrix (in %) for the 10-way QDA model using leave-one-out method

Sample (To) → / (From) ↓	AG 1wk	AG 3wk	AG 5wk	AG 8wk	AN 1wk	AN 3wk	AN 5wk	AN 8wk	Pen 8wk	Healthy
AG 1wk	47	8	0	1	26	14	1	0	2	1
AG 3wk	18	21	3	1	5	43	5	1	1	2
AG 5wk	0	1	39	15	2	0	38	3	2	0
AG 8wk	1	3	8	41	1	2	11	16	17	0
AN 1wk	35	5	1	1	37	11	2	3	0	5
AN 3wk	19	18	0	1	6	50	1	1	2	2
AN 5wk	1	2	32	20	0	1	27	9	6	2
AN 8wk	1	2	3	27	0	4	12	35	15	1
Pen 8wk	0	2	2	15	0	3	3	15	60	0
Healthy	7	0	0	0	17	2	1	0	0	73

Table A.8 Confusion matrix (in %) for the 10-way QDA model using bootstrapping method

Sample (To) → / (From) ↓	AG 1wk	AG 3wk	AG 5wk	AG 8wk	AN 1wk	AN 3wk	AN 5wk	AN 8wk	Pen 8wk	Healthy
AG 1wk	67.1	4.9	0	0	12.2	12.8	1.0	0	1.0	1.0
AG 3wk	16.2	29.8	1.0	1.0	5.0	41.0	3.0	1.0	1.0	1.0
AG 5wk	0.0	1.0	59.8	10.2	2.0	0.0	23.0	2.0	2.0	0.0
AG 8wk	1.0	2.0	6.0	60.2	1.0	1.0	8.1	7.9	12.8	0.0
AN 1wk	25.1	5.1	0.0	0.0	58.1	7.8	1.0	1.0	0.0	0.9
AN 3wk	11.0	9.9	0.0	1.0	5.0	69.0	0.0	1.1	2.0	1.0
AN 5wk	1.0	1.0	14.1	17.8	0.0	1.0	52.1	7.0	4.0	2.0
AN 8wk	1.0	2.0	2.1	20.9	0.0	4.1	9.0	49.9	11.0	0.0
Pen 8wk	0.0	2.0	2.0	9.0	0.0	3.1	2.0	10.8	71.1	0.0
Healthy	6.0	0.0	0.0	0.0	13.1	2.0	1.0	0.0	0.0	78.0

Table A.9 Confusion matrix (in %) for the 5-way QDA model using leave-one-out method

Sample (To) → / (From) ↓	1wk infected	3wk infected	5wk infected	8wk infected	Healthy
1wk infected	69.0	21.5	3.0	2.5	4.0
3wk infected	17.0	72.5	4.0	4.0	2.5
5wk infected	0.5	2.0	75.0	21.5	1.0
8wk infected	2.0	4.3	15.0	78.0	0.7
Healthy	19.0	1.0	2.0	0.0	78.0

Table A.10 Confusion matrix (in %) for the 5-way QDA model using bootstrapping method

Sample (To) → / (From) ↓	1wk infected	3wk infected	5wk infected	8wk infected	Healthy
1wk infected	79.0	17.0	1.5	1.0	1.5
3wk infected	13.4	78.6	2.5	3.0	2.5
5wk infected	0.5	2.0	78.0	18.5	1.0
8wk infected	1.6	4.4	13.1	80.3	0.6
Healthy	18.0	0.0	0.0	0.0	82.0

Table A.11 Confusion matrix (in %) for the 3-way QDA model using leave-one-out method

Sample (To) → / (From) ↓	1 wk			3 wk			5wk			8wk			
	A. glaucus	*A. niger*	Healthy	*A. glaucus*	*A. niger*	Healthy	*A. glaucus*	*A. niger*	Healthy	*A. glaucus*	*A. niger*	Healthy	*Penicillium*
A. glaucus	63.0	36.0	1.0	33.0	60.0	7.0	48.0	51.0	1.0	57.0	25.0	0.0	18.0
A. niger	46.0	48.0	6.0	30.0	66.0	4.0	41.0	57.0	2.0	33.0	44.0	4.0	19.0
Healthy	8.0	18.0	74.0	8.0	6.0	86.0	0.0	5.0	95.0	0.0	1.0	99.0	0.0
Penicillium	-	-	-	-	-	-	-	-	-	19.0	18.0	0.0	63.0

Table A.12 Confusion matrix (in %) for the 3-way QDA model using bootstrapping method

Sample (To) / (From)	1 wk			3 wk			5wk			8wk			
	A. glaucus	*A. niger*	Healthy	*A. glaucus*	*A. niger*	Healthy	*A. glaucus*	*A. niger*	Healthy	*A. glaucus*	*A. niger*	Healthy	*Penicillium*
A. glaucus	85.1	14.0	0.9	45.0	50.9	4.1	68.9	30.1	1.0	73.9	12.0	0.0	14.1
A. niger	32.1	64.9	3.0	15.0	83.0	2.0	16.0	82.0	2.0	26.1	60.9	3.0	10.0
Healthy	7.0	13.0	80.0	6.0	4.0	90.0	0.0	1.0	99.0	0.0	0.0	100.0	0.0
Penicillium	-	-	-	-	-	-	-	-	-	11.0	13.0	0.0	76.0